MICROEVOLUTIONARY PROCESSES UNDERLYING MACROEVOLUTIONARY PATTERNS OF ELECTRIC SIGNAL DIVERSITY IN MORMYRID FISH

Jason R. Gallant*[1], Joshua Sperling[2], Catherine Cheng[2], Matthew E.Arnegard[3], Bruce A. Carlson[4], Carl D. Hopkins[2]

[1]Michigan State University Department of Zoology, East Lansing MI 48824 USA
[2]Cornell University Department of Neurobiology and Behavior, Ithaca NY 14853 USA
[3]Fred Hutchinson Cancer Research Center, Seattle, WA 98109 USA
[4]Washington University in St. Louis Department of Biology, St. Louis, MO 63130 USA

*Author to whom correspondence should be addressed

Abstract

This study examines evolutionary causes underlying the maintenance of diversity in electric courtship signals (EODs) emitted by the mormyrid electric fish species *Paramormyrops kingsleyae*. *P. kingsleyae* are polymorphic for an EOD feature which characterizes interspecific signal diversity among the rapidly diverged *Paramormyrops* genus. We collected 338 specimens and recorded EOD signals from 9 populations distributed throughout Gabon, west central Africa, collected in 1999-2009. First, we demonstrate using microsatellite genotyping a significant signature of isolation by distance between populations. Second, utilizing principal components analysis of 21 landmarks measured from EOD waveforms, we find that EOD duration and the magnitude of a small head negative pre-potential (P0) are highly correlated with patterns of spatial and genetic structure. Finally, utilizing a behavioral assay, we demonstrate that *P. kingsleyae* individuals can discriminate between P0-absent and P0-present EOD waveforms, although genetic and morphological analysis indicate no assortative mating between signal types. Together, these results support the hypothesis that patterns of signal variation in *P. kingsleyae* have resulted from genetic drift acting upon isolated populations. As *P. kingsleyae* represents a microcosm of signal diversity among mormyrids, these findings illustrate a potential mechanism by which interspecific patterns of EOD diversity may originate at the population level.

Introduction

Stabilizing selection acting on courtship signals and the preferences for those signals ensures successful reproduction between potential mates. Disruption of the behavioral coupling between signaler and receiver can increase the probability of reproductive isolation, and eventually speciation (Pillay and Rymer 2012), as evidenced by numerous rapidly evolved groups of species with highly diverse courtship signals (Diamond 1986; Allender et al. 2003; Mendelson and Shaw 2005; Boul et al. 2006; Mullen et al. 2007; Arnegard et al. 2010b). Several models of speciation strongly implicate the evolution of divergent mate choice behavior (or prezygotic mechanisms in general) in the speciation process (Lande 1981; Boughman 2002; Schluter 2009; van Doorn et al. 2009), though it is presently a challenge in speciation research to disentangle the roles of natural selection, sexual selection, and drift in the early evolution of reproductive isolation (Butlin et al. 2012). Resolution of this and other fundamental, questions in speciation hinges on a more detailed understanding of the mechanisms by which communication divergence originates in natural populations in diverse signaling modalities.

To date, detailed understanding of the mechanisms of signal divergence is well understood in only a few model systems (e.g. Maan et al. 2010; Chung et al. 2014; Ryan and Guerra 2014), partly owing to difficulties in understanding the anatomical and physiological substrates of signal generation and perception. In systems where these substrates are at least partly understood, many signaling modalities are constrained by environmental effects on signal transmission and reception (Bradbury and Vehrencamp 2011), resource competition (Kingston and Rossiter 2004), or predation (Ryan 1988), making it difficult to disentangle the relative effects of sexual selection, natural selection

and drift.

Weakly electric fish, such as African mormyrids are ideally suited for overcoming these experimental difficulties. Mormyrids communicate using electric signals termed electric organ discharges (EODs). These signals are highly diverse and are easily measured and quantified; importantly, they have a well-characterized and discrete anatomical and physiological basis related to the function of other electrically excitable tissues such as muscle and nerve (Bennett and Grundfest 1961; Arnegard et al. 2010a; Gallant et al. 2011; Carlson and Gallant 2013). The electric modality, when compared to other signaling modalities, is relatively free from constraint: electric signals travel at the speed of light without distortion from the environment (Hopkins 1999), and by virtue of few other sympatric electroreceptive organisms are relatively private from eavesdropping by predators (Stoddard 1999).

Mormyrids are one of the most rapidly speciating groups of ray-finned fishes (Carlson et al. 2011; Rabosky et al. 2013). There are at least two species radiations of African mormyrids, one in the genus *Campylomormyrus* (Feulner et al. 2007; Feulner et al. 2008) and a second in the genus *Paramormyrops* (Sullivan et al. 2002; Sullivan et al. 2004). There are more than 20 nominal *Paramormyrops* species, which have rapidly diverged in the geographically restricted drainage basins of West-Central Africa. *Paramormyrops* exhibit highly divergent EODs, which vary primarily in duration (0.5-8 ms), the number of phases, and polarity (Fig. 1; Sullivan *et al*. 2000) . Recent work has demonstrated that the evolution of electric signals far outpaces divergence in morphology, size and trophic ecology, implying over broad taxonomic scales that *Paramormyrops* diversification may largely have been driven by evolution of electric

communication (Arnegard et al. 2010b).

This motivates the question of whether evolution of EOD discrimination or evolution of EOD signals is responsible for the divergence of *Paramormyrops*. Carlson et al. (2011) demonstrated that over broad taxonomic scales, evolutionary changes in mormyrid brain regions known to process EOD signals precede the evolution of clades with highly diverse EOD waveforms. This suggests that neural 'innovation' may, at least at macroevolutionary scales, facilitate EOD divergence. Detailed physiological and behavioral data implicate these changes lead to *increased* ability to discriminate fine-scale differences in EOD waveforms (Carlson et al. 2011; Lyons-Warren et al. 2013). The ability for fine-scale discrimination is consistent with profound and rapid diversification of temporal features of *Paramormyrops* EODs (Sullivan et al. 2002; Sullivan et al. 2004), as well as behavioral studies that indicate *Paramormyrops* highly prefer species-specific EOD waveforms (Hopkins and Bass 1981; Arnegard et al. 2006). Together, these findings raise two alternative scenarios. Divergent selection or drift could 1) act on signal preference, exerting divergent selective pressure on EOD waveforms or, 2) could act directly on EOD signals, exerting divergent selective pressure on receivers. Distinguishing between these alternative scenarios would grant considerable insight into the mechanisms of *Paramormyrops* divergence.

The Study System

To better understand how broad macroevolutionary patterns in EOD trait divergence resulted from processes acting among individual populations, Gallant *et al*. (2011) examined patterns of geographic variation among the highly vagile,

geographically widespread *Paramormyrops* species, *P. kingsleyae*. *P. kingsleyae* exhibit clinal variation in EOD signals with regard to duration, and are polymorphic with regard to a small head-negative phase, termed P0 (Fig. 1A). This signal feature is, at maximum, 2% of the peak-to-peak amplitude of some EODs, but is altogether absent in some geographically isolated forms.

Despite this subtle difference in EOD signals, the anatomical substrate for P0-present and P0-absent signals requires a considerable reorganization of the cells that comprise the electric organ (electrocytes). Individuals with P0-present EODs possess electrocytes with penetrating stalks and anterior innervation (type *Pa*) whereas in P0-absent EODs, electrocyte have non-penetrating stalks with posterior innervation (type *NPp*). The majority of populations across Gabon have P0-present EODs (Fig. 2; Gallant et al. 2011), however in several populations in southern Gabon, within a watershed region of the Louétsi river every individual has P0-absent EODs.

Signal diversity in *P. kingsleyae* is a microcosm of signal diversity for the entire *Paramormyrops* species flock, as well as several other mormyrid genera: *NPp* type electric organs, together with their P0-absent EOD waveforms have independently evolved from *Pa* type electric organs at least five times in *Paramormyrops* and seven times within mormyrids (Sullivan et al. 2000; Sullivan et al. 2002; Sullivan et al. 2004), and thus represent one of the major aspects of signal diversity among *Paramormyrops* species.

In this regard, *P. kingsleyae* are ideally suited for distinguishing the relative role of genetic drift and selection in EOD evolution, as well as the relative order in which EOD preference and EOD diversity first arise in populations. In this study, we test the

hypothesis that the contemporary distribution of signals observed in *P. kingsleyae* is best explained by genetic drift acting upon EOD signals as a result of geographic isolation between populations. This hypothesis is based on several lines of evidence. First, Gallant et al. (2011) ruled out several adaptive explanations for intraspecific EOD diversity within *P. kingsleyae* given the small magnitude of phase P0, together with lack of correlated variation in EOD waveform with environmental variables, predators or sympatric species. Second, a previous study provided evidence of substantial genetic partitioning between two allopatric populations of *P. kingsleyae* in southern Gabon (Arnegard et al, 2005), motivating the hypothesis that genetic drift between geographically isolated populations sufficiently explained the pattern of EOD signal variation among *P. kingsleyae*. Third, Gallant et al. (2011) identified two populations, Apassa and Bambomo Creek, in which both signal types occurred. Several morphologically intermediate individuals with both Pa and NPp electrocytes were identified in these populations, and were putatively considered as evidence of hybridization. This suggested that the ability to discriminate EOD waveforms within *P. kingsleyae* did not exist, or that assortative mating did not occur (i.e. no preference for signal type).

To test the overall hypothesis that genetic drift is sufficient to explain patterns of EOD diversity between geographically isolated populations of *P. kingsleyae*, we examined variation in population genetic structure using microsatellite genotyping within and between *P. kingsleyae* populations with divergent EOD signal types across Gabon, and found that EOD variation is highly correlated with patterns of genetic variation between populations. In the second experiment, we assessed the ability of field-captured

and laboratory maintained *P. kingsleyae* to discriminate divergent *P. kingsleyae* EOD waveforms. We found that while *P. kingsleyae* are capable of discriminating the differences between P0-present and P0-absent EODs, our genetic data, bolstered by additional evidence of hybridization in Bambomo and Apassa creeks, did not support EOD waveform preference among *P. kingsleyae*. Together, our data demonstrate that evolutionary changes, facilitated by genetic drift between geographically isolated populations, predates the evolution of mating preferences and may be the earliest steps of divergence between *Paramormyrops* populations.

Materials and Methods

Specimen Collection, EOD Recording, and EOD Analysis

Collections of *Paramormyrops kingsleyae* specimens were made during field trips to Gabon, West Central Africa in 1999, 2001 and 2009 from locations summarized in Table 1 and Figure 2. Fish were collected using a variety of methods, including fish traps baited with worms, hand nets and electric fish detectors, hook and line, and light rotenone applications. Following any application of rotenone, fish were immediately transferred to fresh, aerated water, where they recovered completely. We saw no difference in the EODs of rotenone captured fish and those captured using other methods.

EODs of each specimen were originally recorded within 24 hours of capture in 1- to 5 liter plastic boxes filled with water from the collection site. Signals were recorded with bipolar chlorided silver wire electrodes, and amplified (bandwidth =0.0001-50 kHz) with a differential bioamplifier (CWE, Inc : Ardmore, PA), and digitized at a 100 kHz-1 MHz sampling rate, with head-positivity plotted upward using a Daqbook or WaveBook (IOTECH: Cleveland, OH), or a USB-powered A-D Converter (National Instruments: Austin, TX). All EOD recordings were made at a vertical resolution of 16 bits per

sample. After recording their EODs, individual specimens were euthanized with an overdose of MS-222. We removed one or more paired fins from specimens and preserved these tissues in 95% ethanol. Each specimen was given a unique specimen identification tag, and fixed free-floating in 10% formalin (phosphate-buffered; pH 7.2) for at least 2 weeks. Specimens were then transferred to 70% ethanol, and deposited in the Cornell University Museum of Vertebrates. All methods conform to protocols approved by Cornell University's Center for Research Animal Resources and Education.

Following the methods described by Gallant *et al.* (2011) and by Arnegard *et al.* (2003), we made 21 measurements (see Fig. 3; Table 2) from each recorded EOD waveform using a custom written program in MATLAB (Mathworks, Inc.: Natick, MA). For each waveform, we calculated amplitudes, times, and slopes at nine landmarks defined by peaks, zero crossings, first derivative peaks, and threshold crossings (see Gallant et al (2011); supplemental materials). In addition, we calculated a power spectrum for each EOD waveform using the MATLAB *fft* function to determine the peak frequency and a low and high frequency with power 3 dB below the peak frequency for each EOD recording. We quantified patterns of EOD variation among all the *P. kingsleyae* individuals collected by performing principal components analysis (PCA) on the set of all 21 measurements (normalized by using the MATLAB function *zscore*) using the MATLAB function *princomp*.

Microsatellite Genotyping

We extracted DNA from the ethanol-preserved fin clips using DNeasy Tissue Kits (Quiagen, Inc.) for the 1998-1999 samples, or AgenCourt DNAadvance kits (Beckman-Coulter, Inc) for the 2009 samples. The 1998-1999 DNA samples originally genotyped by Arnegard et al. (2005) were re-genotyped for this study so that genotypes could be

scored using identical criteria. We amplified DNA at each of five microsatellite loci (NBB001-NBB005) originally identified by Arnegard et al. (2005) using the Quiagen Type-It multiplex PCR System (Quiagen, Inc.). Reaction volumes were 15µl, consisting of 1µl template DNA, 7.5µl Type-it Multiplex Master Mix (containing HotStarTaq Plus DNA Polymerase and PCR buffer with 6µM $MgCl_2$), and 2 pmol of each primer (5' primers labeled with Applied Biosystems fluorescent dyes FAM, HEX or NED). Thermal cycling (under mineral oil) was 5 min at 95˚C (initial activation) followed by 28 cycles of 95˚ for 30 sec, 60˚C for 90 sec, and 72˚C for 30 sec. Each individual reaction (containing PCR products for all 5 loci) was resolved by electrophoresis on an ABI 3100 automated sequencer (Applied Biosystems). Under these thermal conditions, reactions for locus NBB004 failed for the Bambomo, Nyamé-Pendé, and Balé Creek populations. For these populations, an additional PCR reaction was performed as above using primers only for the NBB004 locus, with thermal cycling (under mineral oil) for 5 min at 95˚C (initial activation) followed by 35 cycles of 95˚ for 30 sec, 50˚C for 90 sec and 72˚C for 30 sec. Following genotyping, individual fragment lengths were analyzed and binned according to size by visual inspection, using Genemapper 4.1 software (Applied Biosystems).

Genotyping Data Analysis

For each microsatellite locus (NBB001-NBB005), we examined possible deviations from expected Hardy-Weinberg equilibrium within populations using the two-tailed exact test (Weir 1990) as implemented by GENEPOP v4.1 (Rousset 2008). Next, we performed exact tests of linkage disequilibrium between all pairs of loci (within and between populations), to test the independent assortment of loci. Statistical significance in both sets of tests was evaluated using Markov chain methods (10,000 dememorization

steps; 1,000 batches; 5,000 iterations per batch). We additionally calculated observed and expected heterozygosity under Hardy-Weinberg equilibrium for each locus in every population using the software Arlequin 3.5 (Excoffier and Lischer 2010). The significance of each was evaluated at both the p=0.05 α probability threshold and the Bonferroni corrected threshold of p=0.001.

We quantified genetic differentiation between populations using F_{st} (Weir, Cockerham, 1984). This standardized measure of population genetic structure is equivalent to the variance of allele frequencies between populations (i.e., subpopulations, or s) divided by the variance of allele frequencies in the total population consisting of both subpopulations combined (t). We estimated F_{st} values using Arlequin v 3.5 (Excoffier and Lischer 2010). Using the same software, we evaluated the statistical significance of the F_{st} estimates (at both the uncorrected and Bonferroni-corrected thresholds) by permuting genotypes between populations 50,000 times.

In addition to quantifying population genetic differentiation, we also mapped geographic distances between populations to test for patterns of genetic isolation by distance among populations of *P. kingsleyae*. Pairwise distances between all study populations were computed using digitized topographic maps, which were superimposed over satellite imagery provided in Google Earth software (Google, Inc. v.6.0.1). For each pair of populations, the distance between any two populations was assumed to be the shortest river path between the populations. For some pairwise comparisons, these distances traversed a known waterfall, Bongolo Falls, which is a known barrier to direct upstream migration (Fig. 2).

We used a Mantel test, implemented in the program IBD v.1.5.2 (Bohonak 2002),

to test for a correlation between genetic distances (i.e., pairwise F_{st}) and geographic distances. Statistical significance of the correlation was estimated by permuting the data 1,000 times for the Mantel test, which accounts for non-independence of multiple comparisons. Data were then fitted using a reduced major axis regression technique (Bohonak 2002). Confidence intervals around the fitted line were computed by one-delete jackknifing over all populations (Bohonak 2002).

Bayesian Clustering Analysis

We examined the multilocus genotype data for evidence of population structure among all *P. kingsleyae* individuals collected without making *a priori* categorizations by EOD waveform or collection locality. To do so, we used the program *Structure* 2.3 (Pritchard et al. 2000; Falush et al. 2003), which employs a model-based Bayesian clustering algorithm to determine the most probable number of "populations" (K) into which individuals cluster genetically, as well as the probability of each individual's membership in each cluster. All simulations were run under an admixture model, allowing for separate alpha values (a model parameter expressing the degree of admixture) for each population. Otherwise, default parameters were used. Simulations were run with 5 replicates each for each K value from K=1 to K=14, with a 25,000 MCMC iteration burnin followed by 250,000 MCMC iterations for each run. The simulations were performed using a parallel computing version of *Struture* 2.3, provided by the BioHPC Web Computing Resources, via the Cornell University Computational Biology Service Unit.

To determine the appropriate number of clusters (K), we used a method described by Evanno et al. (2005), which detects hierarchical population structure in a given sample. Our initial run detected two clusters, within which we wished to detect further

population substructuring. Following the methods of Evanno et al. (2005), we used each individual's highest probability of membership in each cluster to assign individuals to subgroups. Each subgroup was subsequently analyzed with STRUCTURE to determine the number of clusters it comprised. This process was repeated until no further clusters could be determined for a subgroup (i.e., highest log-likelihood was for K=1). Following each *Structure* analysis, we used the software *Clumpp* (Jakobsson and Rosenberg 2007) to align outputs and determine a mean permuted matrix of individual cluster membership across replicates. This matrix was then visualized using the cluster visualization program *Distruct* (Rosenberg 2004).

Electric Organ Histology & Analysis

Serial sections of electric organs from selected individuals were made for light-microscopy analysis following the methods described by Gallant et al. (2011). Briefly, electric organs were removed from fixed specimens, decalcified overnight, dehydrated in a graded alcohol series, and infiltrated in glycol methacrylate resin (JB-4 resin; Polysciences, Inc). Serial sagittal sections, each 6 µm thick, were cut from lateral to medial with a tungsten carbide microtome knife, mounted on glass slides, and stained with 0.5% Toluidine blue for 30 sec. For each specimen, we reconstructed one of four columns of electrocytes from these serial sections. Because each column of electrocytes surrounds the spinal cord, we began our reconstruction at the lateral edge of the electric organ, and stopped the reconstruction when the spinal cord was clearly visible (approximately 234-648 µm depending on the size of the individual). For each section, the number of stalk penetrations through each electrocyte was counted in, and averaged across, 50-70 electrocytes per section. An electrocyte was scored with a penetration whenever a stalk was observed to pass through either or both faces of the electrocyte.

For our analysis, we considered each 6 µm section to have an independent number of penetrations from all other sections to minimize the probability of underestimating the total number of penetrations.

Behavioral Playback Experiments

We performed two sets of electrical playback experiments to assess the ability of *P. kingsleyae* to discriminate P0-present and P0-absent waveforms. For all experiments, we assessed behavioral discrimination of EOD waveforms using a dishabituation paradigm described in detail by Carlson et al. (2011). Specimens were placed in a rectangular PVC enclosure containing both chlorided silver wire stimulus electrodes (Ag/AgCl) and Ag/AgCl recording electrodes, with the two pairs of electrodes oriented orthogonally with respect to one another. We delivered stimulus trains consisting of 10 bursts of 10 EOD pulses each, with an intra-burst interval of 30 ms, and inter-burst interval of 10 s, with a peak-to-peak intensity of 145 mV/cm. Negative control trains were 10 bursts of identical EOD pulses. Positive control and experimental trains consisted of 8 bursts of identical EODs (background), with the 9th burst consisting of a novel waveform, followed by a 10th burst of the original background waveform. The EOD rate throughout each stimulus was estimated by convolving EOD times with a 300-ms Gaussian waveform (Carlson and Hopkins 2004). The specimen's response was then recorded as the maximum EOD rate within a 2 sec window following each burst of EODs (Carlson et al. 2011). The magnitude of the specimen's response declined over repeated presentation of the background bursts (habituation). Therefore, we measured each specimen's 'novelty response' as the change in EOD discharge rate (dishabituation) following the 9th (novel) burst, relative to the EOD discharge rate following the 8th presentation of the background burst. Using a Dunnett's Test with Control (Dunnett

1955), we compared novelty response toward the positive control stimulus and negative control. Significantly different novelty responses to these experimental trains vs. negative control were considered evidence for discrimination between background and novel waveforms.

Positive control novel EOD stimuli were constructed by phase-shifting the background EOD waveform by 90˚, which is maximally divergent in the time domain while preserving the frequency-spectrum. Phase shifting of EODs was accomplished by performing an FFT on the EOD waveform, followed by adding 90 degrees to the phase angle at each positive frequency, and subtracting 90 degrees from each the phase angle at each negative frequency. This was followed, in turn, by inverse FFT, which yielded a reconstructed EOD characterized by an altered (i.e., 90˚ shifted) phase spectrum with an unaltered power spectrum (Heiligenberg and Altes 1978; Hopkins and Bass 1981; Carlson et al. 2011).

One set of experiments was performed on *P. kingsleyae* specimens within 6 hours of capture from Bambomo (n=10) and Mouvanga creeks (n=10). A second set of experiments was performed on additional P0-absent individuals from Bambomo Creek, which were captured and transported to the Hopkins laboratory at Cornell University (Ithaca, NY) for further study. Fish were housed in community tanks with other individuals captured from their home stream. In addition, the fish were fed live blackworms daily, and they were maintained on a 12-hour light/dark cycle, with water temperatures maintained between 25-27˚C, pH between 6.5-7.0, and water conductivity between 200-400µS.

Results

Loci Attributes, Linkage Equilibria and Hardy-Weinberg Proportions

We were able to amplify fragments without any failed reactions (i.e. possible null homozyogotes) for all 338 individuals genotyped in this study. Total number of alleles detected at each of 5 loci over all populations ranged from 2-21 (Table 3). For each population, locus-specific expected heterozygosities ranged from 0.11-0.88 (Table 3). Exact tests produced no evidence of linked loci across all populations ($p > 0.17$). Of 55 unique locus-by-population combinations, only a few cases exhibited evidence of a deviation of observed heterozygosity from the expectation under Hardy-Weinberg equilibrium (at uncorrected $p=0.05$). The exceptions were NBB002: Balé ($p=0.015$) and Nyamé-Pendé ($p=0.019$); NBB003: Bambomo 1999 ($p=0.003$); NBB004 (Bambomo 1999, Bambomo 2009, and Nyamé-Pendé; all $p<0.0001$); NBB005 (Bikagala $p=0.038$). After Bonferoni adjustment for multiple comparisons, only the NBB004 samples for Bambomo 1999, Bambomo 2009, and Nyamé-Pendé remain significant.

Fig. 4 shows the allele frequency histograms at each of 5 loci for each of the 338 individuals in the full dataset for this study, grouped by population. Two populations at Mouvanga and Bambomo Creeks were sampled in 1999-2001 and again in 2009. Allele frequencies appeared to change little over this 10 year period between sampling. Between populations, there are apparent differences between the distribution of alleles; of particular note are the presence of several alleles (NBB002, ~250 bp, NBB005 several alleles between 300-400 bp), which are present in Bambomo and Apassa creeks but absent in other populations.

Differences in allele frequencies suggest strong genetic differentiation between most

populations of P. kingsleyae

Fig. 5 summarizes F_{st} values of all pairwise comparisons between the *P. kingsleyae* populations surveyed. All populations were significantly differentiated from one another at the p=0.05 and the Bonferonni-corrected threshold (p=0.001), with the exceptional pairwise comparisions of Bambomo Creek 1999 vs. 2009, Mouvanga Creek 1999 vs. 2009, and Nyamé-Pendé vs. Bale Creek. Among all pairs of populations, the magnitude of genetic differentiation between populations varied from F_{st} = 0.06 to F_{st} = 0.65.

Pairwise genetic differentiation between populations is related to geographic distance

Next, we investigated the relationship between genetic differentiation (F_{st}) and geographic distance, measured by shortest river distance between populations (Fig. 6). As described above, we calculated the shortest river distance between each population in every population pair; in some pairs, this distance traversed Bongolo Falls, and in others it did not. We have indicated these populations in Fig. 6 as closed circles and open circles, respectively. Among all population pairs in the South of Gabon, we found a significant relationship between pairwise genetic distance and pairwise geographic distance (Mantel Test Z=720090.47, $p<0.001$; R^2=0.60). We were unable to resolve any differences between population comparisons that traversed the waterfall and those that did not. Two comparisons (Mouvanga Creek 1999 vs. Songou Creek and Mouvanga Creek 2009 vs. Songou Creek) exceeded the 95% CI of this linear regression; in both cases genetic differentiation greatly exceeded the predicted relationship based upon geographic distance.

Bayesian clustering analysis suggests hierarchical population structure that corresponds

to geographic barriers and distance

Hierarchical analysis of population structure for all 338 individuals was performed using Structure 2.3 (Pritchard et al. 2000; Falush et al. 2003), following the method of Evanno et al. (2005). We employed the ΔK approach (Evanno et al. 2005) to determine the lowest hierarchical level of population structure in the dataset containing all populations (K=2). To determine structure of subpopulations, we divided the whole dataset into 2 subpopulations (G1 and G2) based on the most probable assignment of each individual to either group. We then ran STRUCTURE again independently on each subgroup to determine the most likely number of subpopulations in each group. In G1 there were two subgroups (G1.A and G1.B), and in G2, there were three subgroups (G2.A, G2.B, and G2.C). We repeated this procedure of splitting groups and performing structure analysis for each subpopulation until no further structure could be detected (highest likelihood value was for K=1). This resulted in the splitting of G1.B into three additional groups (G3.A, G3.B, and G3.C). Using this method, we detected 3 hierarchical levels of population structure in the total dataset, with 8 distinguishable clusters.

Fig. 7a shows the probability of membership in each cluster of each of the 338 individuals genotyped shown as a bar chart, organized by collection locality over each of the detected hierarchical levels. Considering the highest level of population structure for each group, most individuals were assigned with high confidence to a cluster. With few exceptions, at the highest hierarchical level of population structure (i.e. G2.A-C, G3.A-C), individuals were assigned to clusters that corresponded to their source population with the exception of Bambomo and Apassa (G1.A), which were not further divisible. The lowest levels of hierarchical organization corresponded to major geographic groups

(Fig 7b); G1 was composed of all Southern populations, whereas G2 corresponded to Northern populations and Mouvanga Creek. On the intermediate hierarchical level, G1 was subdivided into G1.A, which corresponded to populations below Bongolo Falls, and G1.B corresponded to populations above Bongolo Falls and Songou Creek.

Patterns of EOD variation relate to signatures of population structure

We assessed variation in EOD signals using principal components analysis for each of the 338 individuals in this study, following the method of Gallant et al., 2011. The first principal component related strongly to duration, and correspondingly explained 41.02% of the variation between individuals. The second factor related strongly to the magnitude of the small, head negative phase P0, and partly to duration, and comprised approximately 17.97% of the variation between electric signals. Factor loadings for these two principal components are summarized in Table 4.

We compared the grouping assignments of each individual from Bayesian clustering analysis described above, to patterns of variation in EOD signals in (Fig 7b). Over the lowest hierarchical level of population structure (Fig. 7b, *upper left*), groups were clearly differentiated in terms of their signals. G1 individuals (Fig. 7b, *upper left, green*) were primarily P0-absent or had small P0s (Apassa Creek) and longer duration, whereas G2 individuals were entirely large magnitude P0-present, and tended to have shorter durations. EOD signals within G2 individuals could further be separated into distinct groups based upon duration and P0 magnitude (Fig. 7b, *upper right*), which corresponded to G2 subgrouping. G1.A individuals (Fig 7b, lower left, *orange*) overlapped with individuals from G1.B (Fig. 7b, *lower left, grey*). Individuals within

G1.A had EODs that had small P0s (primarily from Apassa Creek) as well as EODs that had no P0s (primarily from Bambomo Creek) and varied widely in their duration. G1.B individuals all lacked P0-present EODs, but the three G3 subgroups could be resolved weakly from each other in terms of duration (Fig. 7b, *lower right*).

Morphological Analysis of Electric Organs Identifies Additional Specimens with Mixed Anatomy in Apassa Creek

Gallant et al (2011) showed that P0-absent EODs are produced by fish with NPp anatomy, while P0-present EODs were produced by fish with penetrating stalked electrocytes in the electric organ. In addition, Gallant et al (2011) presented evidence for electric organs with mixed morphology, wherein some electrocytes had penetrating stalks while other electrocytes from the same organ had non-penetrating stalks. We confirmed this observation with an additional analysis of 21 electric organs collected in 2009. Our present analysis supports the existence of these morphological types. In Fig. 8 we show 4 examples of electric organs surveyed in Bambomo, Apassa, Mouvanga, and Songou Creeks, and summarize our analysis of all 21 individuals in Table 5. In Apassa and Mouvanga all individuals were of the Pa morphology type, with one exceptional individual in Apassa exhibiting mixed morphology (*NPp* + *Pa* morphology in the same individual). In Bambomo Creek and Songou creek, we detected individuals that had entirely NPp type morphology, with one exceptional individual in Bambomo creek that had entirely *Pa* type morphology.

P. kingsleyae can detect intraspecific EOD waveform variation

We utilized a habituation/ dishabituation paradigm (Carlson et al. 2011) to determine whether individual *P. kingsleyae* were capable of discriminating between

sympatric and allopatric *P. kingsleyae* EOD waveforms that were either P0-absent or P0-present (Fig. 9A,B). We performed two sets of experiments to assess this: the first set of experiments was performed with single recordings of responses across 20 field-captured individuals (Fig. 9C,D), whereas the second was performed with 5 repetitions of randomly interleaved stimulus trains to laboratory maintained individuals, which enabled us to average responses and thereby reduce variability (Fig 9E-H; see Methods).

In the first field experiment (Fig 9C), *P. kingsleyae* from Bambomo creek showed behavioral evidence of discriminating phase shifted EODs from P0-absent EODs ($p<0.001$), but did not show evidence of discriminating between P0-absent EODs (background) and Mouvanga P0-present EODs or Bambomo P0-present EODs (novel). In the second field experiment (Fig 9A), *P. kingsleyae* from Mouvanga creek showed greater dishabituation to phase shifted EODs than test EODs, but this difference was not significant ($p=0.1751$). There was no significant difference in response between Mouvanga P0-present EODs (background) and Bambomo P0-absent EODs or Bambomo P0-present EODs (novel). Taken together, these field experiments performed on *P. kingsleyae* from Bambomo Creek and Mouvanga creek did not support the hypothesis that *P. kingsleyae* are able to discriminate between the subtly different P0-absent and P0-present waveforms. We therefore performed laboratory experiments that were designed to be more sensitive at detecting small differences in response through averaging.

In the first laboratory experiment (Fig 9E) we tested the hypothesis that *P. kingsleyae* from Bambomo Creek are able to discriminate allopatric P0-present EODs from sympatric P0-absent EODs. We were able to determine a statistically significant response to the positive control (novel=90˚ phase shifted EOD; $p<0.001$). In addition, we

detected statically significant changes in novelty responses to stimulus trains where both Mouvanga P0-present EODs were novel ($p<0.01$), and where Bambomo P0-absent EODs were novel ($p<0.001$). This evidence is consistent with the hypothesis that *P. kingsleyae* are able to discriminate between P0-present and P0-absent waveforms, but is confounded by the fact that allopatric populations, and even individuals, can differ slightly in EOD waveform (see above; Gallant et al., 2011). Thus, there may be cues other than P0 that mediated this discrimination.

To rule out the possibility of individual EOD variation *other than* P0-presence/absence, we tested *P. kingsleyae* captured in Bambomo Creek with individual sympatric EOD waveforms where P0 <u>was not</u> available as a cue (Fig. 9F). Though subjects responded significantly to positive controls ($p<0.001$), subjects did not exhibit a significant novelty response when presented background and novel stimuli that were all P0-absent ($p=0.3478$), or when background and novel stimuli were all P0-present ($p=0.3869$). In a third, corollary laboratory experiment, we tested the hypothesis that *P. kingsleyae* from Bambomo Creek are able to discriminate between sympatrically occurring EOD variants (Fig. 9G) where P0-presence/absence <u>was</u> available as a cue. Subjects responded significantly to positive controls ($p<0.001$), and to P0-present waveforms from Bambomo in a background of P0-absent waveforms from Bambomo ($p=0.02$), though not to P0-present waveforms from Ivindo (which have very large P0s; $p=0.7189$) from a background of P0-absent waveforms. Together, these three experiments support the hypothesis that *P. kingsleyae* can differentiate between sympatric EOD waveforms when P0 is available as a cue.

Finally, in the fourth laboratory experiment (Fig. 9H), we examined the ability of

P. kingsleyae to discriminate between artificial EOD waveforms that had very small P0 peaks present (1:1 P0-absent/P0-present hybrid; see methods), and natural EOD waveforms that had no P0-present. We determined a statistically significant response to positive controls ($p<0.01$), and to EODs that represented 1:3 ratios of P0-absent to P0-present waveforms ($p<0.01$), however, subjects did not elicit a statistically significant response to 3:1 ($p=0.873$) or 1:1 ratios ($p=1.0$) of P0-absent to P0-present EODs.

The results of the field and laboratory experiments are consistent with the hypothesis that *P. kingsleyae* can differentiate between P0-absent and P0-present waveforms.

Discussion

Gallant et al. (2011) considered several alternative hypotheses to explain the observed patterns of variation in *P. kingsleyae* EODs, including various selective pressures (conspicuity to predators, reproductive character displacement, and effects on electrolocation performance), as well as the possibility of reproductive isolation between *P. kingsleyae* signal types. Many of these explanations were considered unlikely, given the small difference in EOD signal between P0-absent and P0-present waveforms, despite the considerable anatomical reorganization of the electric organ. The evidence remaining favored the null hypothesis that genetic drift between geographically isolated populations may have contributed to this divergence alone. We made three predictions from this hypothesis: (1) evidence of genetic structure between populations should be strongly correlated with geography, (2), that geographic and genetic variation should be strongly correlated with variation in EOD signals, and (3) that there should be no

evidence of assortative mating between *P. kingsleyae* EOD types. We consider our evidence for each in turn, before considering the results of our behavioral experiments, which shed light on the significance of our overall findings.

Genetic structure is associated with physical barriers and large distances between populations

We detected significant signatures of pairwise differentiation between all 9 populations compared using F_{st}. The magnitude of differentiation was variable, reflecting populations such as Bambomo and Apassa, which were weakly differentiated (Fst < 0.07) to populations that were strongly differentiated, such as Mouvanga and Soungou creeks (F_{st} >0.6). As noted in Table 3, locus-specific heterozygosities were variable among populations of *P. kingsleyae*. As F_{st} is a ratio of variation between subpopulations to total variation, some of the pairwise comparisons of F_{st} (i.e. Mouvanga Creek vs. Songou Creek) may have been larger than others due to comparisons between two low-heterozygosity populations (discussed in detail below; see also Hedrick 2005).

Overall variation in F_{st} led us to suspect that differences in genetic variation between populations corresponded to reduced gene flow between populations, as would be predicted by "isolation-by-distance" models (Wright 1943). Over relatively short (<120 km) distances in the South of Gabon, where sampling was high, we were able to determine a significant relationship between genetic differentiation (i.e. F_{st}) and geographic distance (i.e. river distances between populations). In our analysis, we incorporated measurements that included pairwise distances that traversed waterfalls, as well as pairwise distances that did not traverse waterfalls. We would expect that

waterfalls, if they acted as barriers between populations should increase genetic distance for a given geographic distance. From Fig. 6, we can see no apparent differences in populations that traversed waterfalls vs. those that did not. Only two comparisons were more differentiated genetically than would have been expected by our regression model, given their geographic proximity: Mouvanga and Songou Creek. Our overall analysis of pairwise F_{st} presents a fairly robust and important conclusion: namely that most allopatric populations of *P. kingsleyae* are strongly genetically differentiated from each other, suggesting overall very low levels of gene flow between populations. Over distances less than 120 km, the amount of gene flow between populations is proportional to the distance between them, consistent with a classic isolation-by-distance pattern of dispersal between populations.

We noted above that this relationship was not apparent over distances greater than 120 km. This common phenomenon is related to the balance between mutational processes within populations and gene flow between them (Hutchison and Templeton 1999). This issue was not limited to geographical distance: some F_{st} values determined in this analysis exceeded previously reported F_{st} values between nominal *Paramormyrops* species by Arnegard et al. (2005), which, measured in sympatry were equal to 0.3 or lower.

In either case as the "distance" (geographic or phylogenetic) between two populations increase, signal related to gene flow (i.e. similarity by descent) decreases relative to the signatures of genetic drift caused by mutational processes in genetic markers. This is a common limitation of microsatellites, which have very high mutation rates and unique mutational processes (Selkoe and Toonen 2006), which make them ideal

for assessing the degree of gene flow between populations when gene flow is high relative to the influences of genetic drift in differentiation. However, as gene flow decreases with distance (as would be expected under IBD models or between two reproductively isolated species), mutational processes contribute a much larger effect to differentiation than does gene flow. As such, the desired signal of similarity by descent becomes confounded by genetic drift. Genetic drift might confound our estimates of F_{st} as a measure of gene flow in two ways: (1) mutations in different populations to the same alleles (i.e. homoplasy) would reduce F_{st} or (2) decreases in heterozygosity through the fixation of alleles due to random genetic sampling would increase estimates of F_{st} (Hedrick, 2005). For these reasons, F_{st} based estimation of population structure by itself seems less than ideal, particularly because it appears to perform poorly at estimating differentiation between populations that are near complete reproductive isolation (i.e. at non-equlibrium states; Hutchison and Templeton 1999), or between populations that have very low heterozygosity.

To circumvent the limitations of using the F_{st} method to assess population structure, we employed a Bayesian clustering analysis of population structure using the program STRUCTURE, which gives an independent, but complimentary picture of population structure by calculating the probability of membership of individuals to a pre-selected number of clusters, assuming clusters are at Hardy-Weinberg equilibrium and exhibit linkage equilibrium (Pritchard et al. 2000). By using the method of Evanno et al. (2005), we could extend this analysis of population structure to gather additional information about hierarchical population structuring that might have resulted from geographic barriers to migration over various regional scales. Overall, STRUCTURE

results were consistent with F_{st} measures of population structure. All populations that had significant F_{st} values were detected as independent structure "clusters" at the highest level of hierarchical organization with nearly 100% probability (Fig. 7), with the exception of Bambomo and Apassa creeks which STRUCTURE could not sort into two distinct groups. Pairwise F_{st} between Bambomo and Apassa was, relative to other populations, very low (< 0.06), but was statistically significant.

In addition, the hierarchical method of Evanno et al. (2005) revealed that *P. kingsleyae* populations are more similar genetically within watersheds than between them, which extends from the regional level (e.g. Northern vs. Southern populations; Fig. 7 G1 vs. G2), down to the local levels (above vs. below Bongolo Falls G1.A vs. G1B). This is overall consistent with the pattern of isolation by distance pattern observed by comparing F_{st} values with geographic distance in Southern populations, albeit over larger geographic scales. These analyses together strongly indicate that gene flow between populations is limited by dispersal between geographically distant populations. While isolation by distance plots showed little effect of the waterfall on gene flow (Fig. 6), the barrier to gene flow caused by Bongolo Falls was visible through STRUCTURE results.

Genetic and geographic structure correlates with detectable patterns of variation in EOD signals.

A key prediction of our hypothesis was that population structure should be highly correlated with patterns of signal divergence. As such, we predicted that patterns of signal diversity are related to signatures of genetic structure. We assessed signal variation as in Gallant et al. (2011) using principal components analysis of 21 variables

derived from 9 EOD landmarks. As in the previous analysis, principal component 1 corresponded primarily to duration and principal component 2 corresponded primarily to the magnitude of peak P0, which is absent in many of the southern populations. Using only these two components of signal variation (which explain ~ 60% of the total variation among EOD waveforms, we examined how genetic structure (as assessed through Bayesian clustering analysis discussed above) and signal differentiation corresponded. Together, our use of the F_{st}, STRUCTURE, and principal component analysis of EOD signals present a consistent picture of genetic and phenotypic differentiation of *P. kingsleyae* EOD waveforms that corresponds strongly to distances between populations, and the presence of waterfall barriers. Over the lowest level of hierarchical analysis, both genotypes and EOD phenotypes were the most divergent. Over the highest levels of hierarchical analysis (i.e. populations in G3.A-C), EODs overlapped more in principal component space, but were still distinguishable. These observations are consistent with populations sharing common ancestry between Northern and Southern populations much earlier than between populations surrounding Bongolo Falls.

No evidence for assortative mating between P. kingsleyae signal types

Several lines of evidence from this and Gallant et al. (2011) strongly support a lack of assortative mating between *P. kingsleyae* types. The strongest evidence comes from our consideration of Bambomo and Apassa creeks, two populations where both signal types occur in sympatry. Despite their relative proximity in our study (ca. 25 km of river distance), the populations *Pa* electric organs with P0-present EODs occur predominantly in Apassa, whereas *NPp* type electric organs with P0-absent EODs are

predominant in Bambomo. Despite these phenotypic differences, F_{st} values indicated that the populations are weakly differentiated, and STRUCTURE analysis was unable to differentiate between the two populations. This demonstrates that there is relatively substantial gene flow between the two populations, despite the fact that they are nearly "fixed" for alternate electric organ anatomies and signal types.

This finding predicts the potential existence of hybrid individuals, which are likely those individuals with mixed morphology in Apassa creek (Fig. 8, in addition to those already discovered in Bambomo Creek (Gallant et al., 2011). A second, genetic line of evidence, is that Bambomo creek and Apassa creek exhibit a so-called "rare alleles" phenomenon (Fig. 4): both populations have additional alleles that are absent from all other populations genotyped, which has been demonstrated as a signature of hybrid zones in other taxa (Golding 1983; Barton 1985; Hoffman and Brown 1995). A final line of evidence comes from biogeography. Fig. 2 illustrates the close proximity between streams that drain above Bongolo Falls, Apassa Creek's headwater, and the headwater branches of Bambomo Creek. Given the large fluctuations in water level due to rainy season (Arnegard et al. 2006), it is entirely plausible that these waterways are periodically connected, allowing migration to occur between these otherwise geographically isolated populations. It is notable that this is precisely the time that breeding in *P. kingslyeaye* (and other mormyrids) occurs.

To summarize, our results suggest that divergent EOD forms in *P. kingsleyae* have likely evolved due to genetic drift between geographically isolated populations. Such substantial population structure is likely generated by two interacting factors: (1) the habitat preferences of *P. kingsleyae* for small headwater streams (Gallant et al. 2011)

and (2) landscape, which is partly imposed by barriers to migration, such as the presence of waterfalls, as well as the physical structure of West-African drainage systems.

How genetic drift may have acted among *P. kingsleyae* populations to generate EOD diversity remains an open question. We have found very little evidence that genetic drift affects the distribution of microsatellite allele frequencies over 10 years of sampling in Bambomo Creek and Mouvanga Creek (Pollack's Fk = 0.02 in Bambomo Creek and 0.019 in Mouvanga Creek). Estimates of effective population size based on these changes in allele frequency imply very large contemporary population sizes (Waples 1989). We note, however our failure to detect small contemporary effective population sizes should not be interpreted that effective population sizes were not historically small, as might be predicted during so-called "founder events" (Mayr 1942). Small effective population sizes resulting from founder events would be a means by which new phenotypes could become rapidly fixed in isolated populations. One potential genetic signature of possible founder events may be the considerable variation in the heterozygosity at several loci among some populations (Table 3).

P. kingsleyae are capable of discriminating variation in EOD Signals

The lack of evidence for assortative mating motivates two alternative potential explanations: (1) *P. kingsleyae* cannot discriminate between signal types, or (2) *P. kingsleyae* are capable of discriminating but do not utilize this information in mate selection. To delineate between these alternatives, we performed behavioral experiments to assess the abilities of *P. kingsleyae to* discriminate EOD signals. Our laboratory experiments demonstrated that *P. kingsleyae* populations *on average* are able to

discriminate between waveforms, both between allopatric (Fig. 9C) and sympatric (Fig. 9E) instances of EOD diversity, though curiously not between more divergent allopatric EOD waveforms (Ivindo, Fig. 9E). Our field and laboratory results together highlight that there is considerable variation between individuals (Fig 9A) in the ability to discriminate between EOD waveforms, suggesting that some individuals may be more capable than others at performing the dishabituation task. Based on several studies that have characterized the neural encoding of EOD waveforms (Amagai et al. 1998; Friedman and Hopkins 1998; Xu-Friedman and Hopkins 1999; Carlson 2009; Carlson et al. 2011; Baker et al. 2013; Lyons-Warren et al. 2013), we originally predicted that *P. kingsleyae* would be incapable of encoding P0-presence/absence differences of such small magnitude, clearly emphasizing the need for additional physiological studies on EOD encoding.

We conclude by noting that *P. kingsleyae* represents a "microcosm" of signal diversity within the *Paramormyrops*. The major components of EOD variation within *P. kingsleyae*, namely duration and in the presence or absence of phase P0, are the same components of variation within *Paramormyrops,* of which more than 20 nominal species have radiated rapidly in West-Central Africa. Field and laboratory playback experiments in *Paramormyrops* reveal strong preferences for species-specific EOD waveforms (Hopkins and Bass, 1981) during courtship. Our data suggest that divergence in both duration and in the presence or absence of P0 can quickly change at the population level resulting from the effects of genetic drift. While genetic drift is considered unlikely to act to drive speciation on its own (Coyne and Orr 2004), interest in genetic drift as an important force in speciation has recently witnessed a resurgence in interest from both a

theoretical and empirical standpoint as it may work in tandem with sexual selection (Tazzyman and Iwasa 2009; Uyeda et al. 2009; Bush and Schul 2010; Runemark et al. 2010).

Intriguingly, our data demonstrate that *P. kingsleyae* appear capable of discriminating between these subtly different EODs, but do not appear to have any preference for signals resulting in assortative mating. Arnegard *et al.* (2010b) recently demonstrated that the evolution of electric signals far outpaces divergence in morphology, size and trophic ecology, implying over broad taxonomic scales, *Paramormyrops* diversification may largely have been driven by evolution of electric signals, however the source of variation upon which selection acts is presently unknown. Carlson et al (2011) suggests over broad taxonomic scales brain evolution in regions encoding temporal differences in EODs precedes EOD diversification. Our behavioral results are consistent with these findings, demonstrating that *P. kingsleyae* are capable of discriminating between remarkably similar EODs.

Assuming that historical processes operating within other *Paramormyrops* lineages reflect similar processes operating within populations of *P. kingsleyae*, our results demonstrate that the earliest stages of divergence in *Paramormyrops* populations may be in EOD signals, not in signal preferences, and emphasize the interaction of unique riverine biogeography and strong habitat preferences, which genetically structure populations to accumulate phenotypic differences upon which selection can later act Under this scenario selection acting on mate choice behaviors within *Paramormyrops* could have the effect of (1) further strengthening phenotypic differentiation, and (2) directly causing or reinforcing reproductive isolation.

Acknowledgments

Permits to collect fishes in Gabon and export them for this study were granted by l'Institut de Recherche en Ecologie Tropicale, l'Institut de Recherches Agronomiques et Forestie`res and the Centre National de la Recherche Scientifique et Technologique. We are grateful for the valuable assistance and logistical support we received from J. D. Mbega and students working in these institutions. All techniques used are in accordance with protocols approved by Cornell University's Center for Research Animal Resources and Education (CARE). Additionally, we thank A. McCune and K. Shaw, J. Fetcho, D. Deitcher, S. Mullen well as two anonymous reviewers for comments on earlier versions of this manuscript. This work was supported by NIMH TG T32 MH015793 and NIH TG 2T32GM007469 to JRG, NIH RO1-DC6206 and NSF 0818305 to CDH, and NSF 0818390 to BAC.

References

Allender, C. J., O. Seehausen, M. E. Knight, G. F. Turner, and N. Maclean. 2003. Divergent selection during speciation of Lake Malawi cichlid fishes inferred from parallel radiations in nuptial coloration. PNAS 100:14074-14079.

Amagai, S., M. Friedman, and C. Hopkins. 1998. Time coding in the midbrain of mormyrid electric fish. I. Physiology and anatomy of cells in the nucleus exterolateralis pars anterior. JOURNAL OF COMPARATIVE PHYSIOLOGY A-NEUROETHOLOGY SENSORY NEURAL AND BEHAVIORAL PHYSIOLOGY 182:115-130.

Arnegard, M., D. Zwickl, and Y. Lu. 2010a. Old gene duplication facilitates origin and diversification of an innovative communication system—twice. Proceedings of the ….

Arnegard, M. E., S. M. Bogdanowicz, and C. D. Hopkins. 2005. Multiple cases of striking genetic similarity between alternate electric fish signal morphs in sympatry. Evolution 59:324-343.

Arnegard, M. E. and C. D. Hopkins. 2003. Multivariate analysis of electric signal variation among seven blunt-snouted Brienomyrus species (Teleostei: Mormyridae) from Gabon. Environmental Biol. of Fishes 67:321-339.

Arnegard, M. E., B. S. Jackson, and C. D. Hopkins. 2006. Time-domain signal divergence and discrimination without receptor modification in sympatric morphs of electric fishes. The Journal of experimental biology 209:2182-2198.

Arnegard, M. E., P. B. McIntyre, L. J. Harmon, M. L. Zelditch, W. G. R. Crampton, J. K. Davis, J. P. Sullivan, S. Lavoué, and C. D. Hopkins. 2010b. Sexual signal evolution outpaces ecological divergence during electric fish species radiation. Evolution Int J Org Evolution 176:335-356.

Baker, C., T. Kohashi, A. Lyons-Warren, X. Ma, and B. Carlson. 2013. Multiplexed temporal coding of electric communication signals in mormyrid fishes. J Exp Biol 216:2365-2379.

Barton, N. 1985. Analysis of hybrid zones. Annual Review of Ecology and Systematics.

Bennett, M. V. L. and H. Grundfest. 1961. Studies on morpology and electrophysiology of electric organs III. Electrophysiology of electric organs in mormyrids. Bioelectrogenesis (C. Chagas and A. Paes de Carvalho, Eds.):113-135.

Bohonak, A. J. 2002. IBD (Isolation by Distance): a program for analyses of isolation by distance. Journal of Heredity 93:153-154.

Boughman, J. W. 2002. How sensory drive can promote speciation. Trends in Ecology & Evolution 17:571-577.

Boul, K. E., W. Chris Funk, C. R. Darst, D. C. Cannatella, and M. J. Ryan. 2006. Sexual selection drives speciation in an Amazonian frog. Proceedings of the Royal Society B: Biological Sciences 274:399-406.

Bradbury, J. W. and S. L. Vehrencamp. 2011. Principles of Animal Communication. Sinauer Associates, Inc.

Bush, S. L. and J. Schul. 2010. Evolution of novel signal traits in the absence of female preferences in *Neoconocephalus* katydids (Orthoptera, Tettigoniidae). PLOS One 5:e12457.

Butlin, R., A. Debelle, C. Kerth, R. R. Snook, L. W. Beukeboom, R. F. C. Cajas, W. Diao, M. E. Maan, S. Paolucci, F. J. Weissing, L. van de Zande, A. Hoikkala, E. Geuverink, J. Jennings, M. Kankare, K. E. Knott, V. I. Tyukmaeva, C. Zoumadakis, M. G. Ritchie, D. Barker, E. Immonen, M. Kirkpatrick, M. Noor, C. M. Garcia, T. Schmitt, M. Schilthuizen, and M. C. S. Network. 2012. What do we need to know about speciation? Trends in Ecology & Evolution 27:27-39.

Carlson, B. A. 2009. Temporal-Pattern Recognition by Single Neurons in a Sensory Pathway Devoted to Social Communication Behavior. Journal of Neuroscience 29:9417-9428.

Carlson, B. A. and J. R. Gallant. 2013. From Sequence to Spike to Spark: Evo-devo-neuroethology of Electric Communication in Mormyrid Fishes. Journal of Neurogenetics 27:106-129.

Carlson, B. A., S. M. Hasan, M. Hollmann, D. B. Miller, L. J. Harmon, and M. E. Arnegard. 2011. Brain evolution triggers increased diversification of electric fishes. Science 332:583-586.

Carlson, B. A. and C. D. Hopkins. 2004. Stereotyped temporal patterns in electrical communication. Anim Behav 68:867-878.

Chung, H., D. W. Loehlin, H. D. Dufour, K. Vaccarro, J. G. Millar, and S. B. Carroll. 2014. A Single Gene Affects Both Ecological Divergence and Mate Choice in Drosophila. Science 343:1148-1151.

Coyne, J. A. and H. A. Orr. 2004. Speciation. Sinauer Associates, Sunderland, MA.

Diamond, J. 1986. Biology of Birds of Paradise and Bowerbirds. Annual Reviews in Ecology and Systematics 17:17-37.

Dunnett, C. W. 1955. A multiple comparison procedure for comparing several treatments with a control. Journal of the American Statistical Association 50:1096–1121.

Evanno, G., S. Regnaut, and J. Goudet. 2005. Detecting the number of clusters of individuals using the software STRUCTURE: a simulation study. Molecular Ecology 14:2611-2620.

Excoffier, L. and H. E. L. Lischer. 2010. Arlequin suite ver 3.5: a new series of programs to perform population genetics analyses under Linux and Windows. Molecular Ecology Resources 10:564-567.

Falush, D., M. Stephens, and J. K. Pritchard. 2003. Inference of population structure: extensions to linked loci and correlated allele frequencies. Genetics 164:1567-1587.

Feulner, P., F. Kirschbaum, and R. Tiedemann. 2008. Adaptive radiation in the Congo River: An ecological speciation scenario for African weakly electric fish (Teleostei; Mormyridae; Campylomormyrus). JOURNAL OF PHYSIOLOGY-PARIS 102:340-346.

Feulner, P. G. D., F. Kirschbaum, V. Mamonekene, V. Ketmaier, and R. Tiedemann. 2007. Adaptive radiation in African weakly electric fish (Teleostei: Mormyridae: Campylomormyrus): a combined molecular and morphological approach. Journal of Evolutionary Biology 20:403-414.

Friedman, M. A. and C. D. Hopkins. 1998. Neural substrates for species recognition in the time-coding electrosensory pathway of mormyrid electric fish. The Journal of neuroscience : the official journal of the Society for Neuroscience 18:1171-1185.

Gallant, J. R., M. E. Arnegard, J. P. Sullivan, B. A. Carlson, and C. D. Hopkins. 2011.

Signal variation and its morphological correlates in *Paramormyrops kingsleyae* provide insight into evolution of electrogenic signal diversity in mormyrid fish. Journal of Comparative Physiology A.
Golding, G. 1983. Increased number of alleles found in hybrid populations due to intragenic recombination. Evolution; international journal of organic evolution.
Hedrick, P. W. 2005. A standardized genetic differentiation measure. Evolution 59:1633-1638.
Heiligenberg, W. and R. A. Altes. 1978. Phase sensitivity in electroreception. Science 199:1001-1004.
Hoffman, S. M. G. and W. M. Brown. 1995. The molecular mechanism underlying the "rare allele phenomenon" in a subspecific hybrid zone of the California field mouse, *Peromyscus californicus*. Journal of Molecular Evolution 41.
Hopkins, C. D. 1999. Design features for electric communication. Journal of Experimental Biology 202:1217-1228.
Hopkins, C. D. and A. Bass. 1981. Temporal coding of species recognition signals in an electric fish. Science 212:85-87.
Hutchison, D. and A. Templeton. 1999. Correlation of pairwise genetic and geographic distance measures: inferring the relative influences of gene flow and drift on the distribution of genetic variability. Evolution:1898-1914.
Jakobsson, M. and N. A. Rosenberg. 2007. CLUMPP: a cluster matching and permutation program for dealing with label switching and multimodality in analysis of population structure. Bioinformatics 23:1801-1806.
Kingston, T. and S. J. Rossiter. 2004. Harmonic-hoppin in Wallacea's bats. Nature 429:654-657.
Lande, R. 1981. Models of Speciation by Sexual Selection on Polygenic Traits. P Natl Acad Sci-Biol 78:3721-3725.
Lyons-Warren, A., T. Kohashi, S. Mennerick, and B. Carlson. 2013. Detection of submillisecond spike timing differences based on delay-line anti-coincidence detection. Journal of Neurophysiology 110:2295-2311.
Maan, M. E., O. Seehausen, and J. J. M. Van Alphen. 2010. Female mating preferences and male coloration covary with water transparency in a Lake Victoria cichlid fish. Biol J Linn Soc 99:398-406.
Mayr, E. 1942. Systematics and the origin of species: from the viewpoint of a zoologist. Columbia University Press, New York.
Mendelson, T. C. and K. L. Shaw. 2005. Rapid speciation in an arthropod. Nature 433:375.
Mullen, S. P., T. C. Mendelson, C. Schal, and K. L. Shaw. 2007. Rapid evolution of cuticular hydrocarbons in a species radiation of acoustically diverse hawaiian crickets (gryllidae: trigonidiinae: laupala). Evolution; international journal of organic evolution 61:223-231.
Pillay, N. and T. L. Rymer. 2012. Behavioural divergence, interfertility and speciation: A review. Behav Process 91:223-235.
Pritchard, J. K., M. Stephens, and P. Donnelly. 2000. Inference of population structure using multilocus genotype data. Genetics 155:945-959.
Rabosky, D. L., F. Santini, J. Eastman, S. Smith, B. Silauskas, J. Chang, and M. Alfaro. 2013. Rates of speciation and morphological evolution are correlated across the

largest vertebrate radiation. Nature Communications 4.
Rosenberg, N. A. 2004. DISTRUCT: a program for the graphical display of population structure. Molecular Ecology Notes 4:137-138.
Rousset, F. 2008. GENEPOP'007: a complete re-implmentation of the GENEPOP software for windows and linux. Molecular Ecology Resources 8:103-106.
Runemark, A., B. Hansson, P. Pafilis, E. D. Valakos, and E. I. Svensson. 2010. Isalnd biology and morphological divergence of the Skyros wall lizard *Podarcis gaigeae*: a combined role for local selection and genetic drift on color morph frequency divergence? BMC Evolutionary Biology 10.
Ryan, M. J. 1988. Constraints and Patterns in the Evolution of Anuran Acoustic Communication *in* B. Fritzsch, ed. The Evolution of the Amphibian Auditory System. Wiley & Sons, Inc.
Ryan, M. J. and M. A. Guerra. 2014. The mechanism of sound production in túngara frogs and its role in sexual selection and speciation. Current Opinion in Neurobiology 28:54-59.
Schluter, D. 2009. Evidence for Ecological Speciation and Its Alternative. Science 323:737-741.
Selkoe, K. A. and R. J. Toonen. 2006. Microsatellites for ecologists: a practical guide to using and evaluating microsatellite markers. Ecology Letters 9:615-629.
Stoddard, P. K. 1999. Predation enhances complexity in the evolution of electric fish signals. Nature 400:254-256.
Sullivan, J. P., S. Lavoué, M. E. Arnegard, and C. D. Hopkins. 2004. AFLPs resolve phylogeny and reveal mitochondrial introgression within a species flock of African electric fish (Mormyroidea: Teleostei). Evolution 58:825-841.
Sullivan, J. P., S. Lavoue, and C. D. Hopkins. 2000. Molecular systematics of the African electric fishes (Mormyroidea: teleostei) and a model for the evolution of their electric organs. The Journal of experimental biology 203:665-683.
Sullivan, J. P., S. Lavoué, and C. D. Hopkins. 2002. Discovery and phylogenetic analysis of a riverine species flock of African electric fishes (Mormyridae: Teleostei). Evolution 56:597-616.
Tazzyman, S. J. and Y. Iwasa. 2009. Sexual selection can increase the effect of random genetic drift-- a quantitative genetic model of polymorphisim in *Oophaga pumilio*, the strawberry poison-dart frog. Evolution 64:1719-1728.
Uyeda, J. C., S. J. Arnold, P. A. Hohenlohe, and L. S. Mead. 2009. Drift promotes speciation by sexual selection. Evolution 63:583-594.
van Doorn, G. S., P. Edelaar, and F. J. Weissing. 2009. On the Origin of Species by Natural and Sexual Selection. Science 326:1704-1707.
Waples, R. S. 1989. A generalized approach for estimating effective population size from temporal changes in allele frequency. Genetics 121:379-391.
Weir, B. S. 1990. Genetic data analysis: methods for discrete population genetic data. Sinauer, Sunderland, MA.
Wright, S. 1943. Isolation by distance. Genetics 28:114-138.
Xu-Friedman, M. and C. Hopkins. 1999. Central mechanisms of temporal analysis in the knollenorgan pathway of mormyrid electric fish. Journal of Experimental Biology 202:1311.

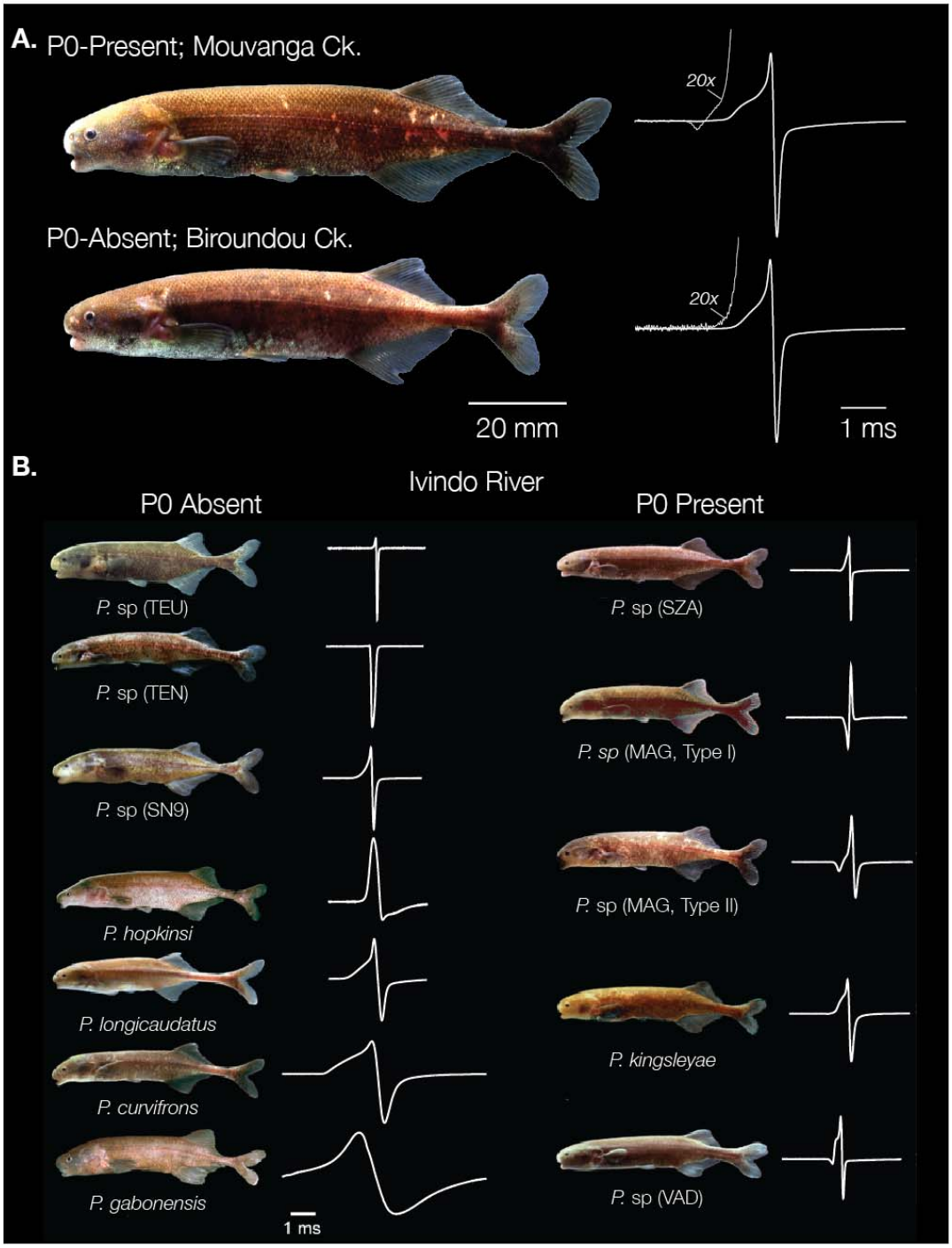
A.
P0-Present; Mouvanga Ck.
20x
P0-Absent; Biroundou Ck.
20x
20 mm
1 ms
B.
Ivindo River
P0 Absent
P0 Present
P. sp (TEU)
P. sp (TEN)
P. sp (SN9)
P. hopkinsi
P. longicaudatus
P. curvifrons
P. gabonensis
1 ms
P. sp (SZA)
P. sp (MAG, Type I)
P. sp (MAG, Type II)
P. kingsleyae
P. sp (VAD)

Figure 1. *Paramormyrops kingsleyae* EOD variation is a microcosm of EOD variation in *Paramormyrops*. A. *P. kingsleyae* EODs are variable in the presence of a small head negative phase (P0), see Gallant et al. (2011). B. 12 sympatric *Paramormyrops* specimens captured from the same locality in the Ivindo River illustrates EOD variation within *Paramormyrops*, which are variable in terms of duration and polarity, as well as in the number of phases. All *Paramormyrops* on the left have P0-absent EOD waveforms, all *Paramormyrops* on the right have P0-present waveforms.

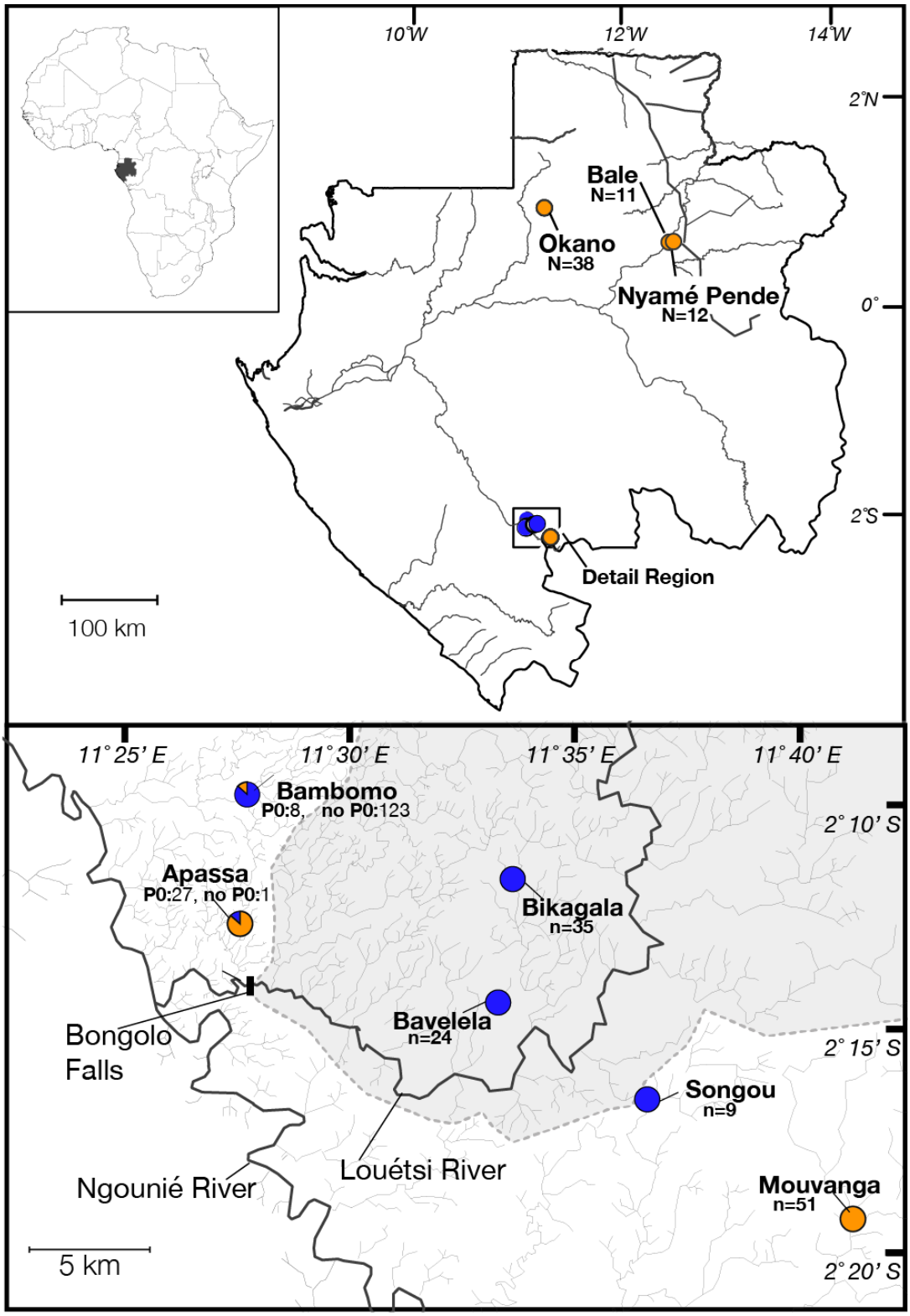
10°W
12°W
14°W
2°N
0°
2°S
Bale
N=11
Okano
N=38
Nyamé Pende
N=12
Detail Region
100 km
11° 25' E
11° 30' E
11° 35' E
11° 40' E
2° 10' S
2° 15' S
2° 20' S
Bambomo
P0:8, no P0:123
Apassa
P0:27, no P0:1
Bikagala
n=35
Bavelela
n=24
Songou
n=9
Mouvanga
n=51
Bongolo
Falls
Ngounié River
Louétsi River
5 km

Figure 2. Map of study populations. Top map shows relationship between populations across Gabon. Box in the south indicates the location of the higher detail map, which indicates the relationship of Southern populations near the confluence of the Louétsi and Ngounié rivers. For all maps, populations are indicated by pie charts, as reported in Gallant et al. 2011. Orange indicates proportion of individuals P0-present, blue indicates proportion of individuals that were P0-absent. Bongolo falls is indicated in the map of southern populations, and a grey region bounded by a dotted line indicates the small streams and creeks that drain into the Louétsi river above Bongolo Falls.

Pop	Year	Lat	Long	N	Genotype	Structure	IBD	EOD	EO	Behavior
Apassa	2009	2° 12' 42'' S	11° 27' 50'' E	28	**X**	**X**	**X**	**X**	**X (4)**	
Bale	2001	0° 31' 9'' S	12° 47' 58'' E	11	**X**	**X**		**X**		
Bambomo	2009	2° 9' 49'' S	11° 27' 42'' E	106	**X**	**X**	**X**	**X**	**X (7)**	**X (17)***
Bambomo	1999	2° 9' 49'' S	11° 27' 42'' E	25	**X**	**X**	**X**	**X**		
Bavavela	2009	2°14' 33''S	11° 33' 22'' E	24	**X**	**X**	**X**	**X**		
Bikagala	2009	2° 11' 43'' S	11° 33' 40'' E	29	**X**	**X**	**X**	**X**		
Mouvanga	2009	2° 19' 23'' S	11° 41' 18'' E	32	**X**	**X**	**X**	**X**	**X (6)**	**X (10)***
Mouvanga	1999	2° 19' 23'' S	11° 41' 18'' E	19	**X**	**X**	**X**	**X**		
Nyame Pende	2001	0° 30' 16'' S	12° 47' 48'' E	12	**X**	**X**		**X**		
Okano	2001	0° 48' 57'' S	11° 39' 1'' E	38	**X**	**X**		**X**		
Songou	2009	2° 16' 42'' S	11° 36' 41'' E	9	**X**	**X**	**X**	**X**	**X (4)**	

Table 1. Summary of locations and years of population samples, and analyses performed on each population.
* Indicates additional individuals were sampled from these populations to perform these analyses. Numbers in parentheses indicate sample sizes, if no sample size is reported, the entire N reported was analyzed. Column IBD indicates populations used in isolation by distance analysis (see methods), Column EOD indicates population used in EOD analysis (see methods). Column EO indicates population utilized in histological analysis of electric organs (see methods). Behavior indicates population utilized in EOD discrimination task (see methods).

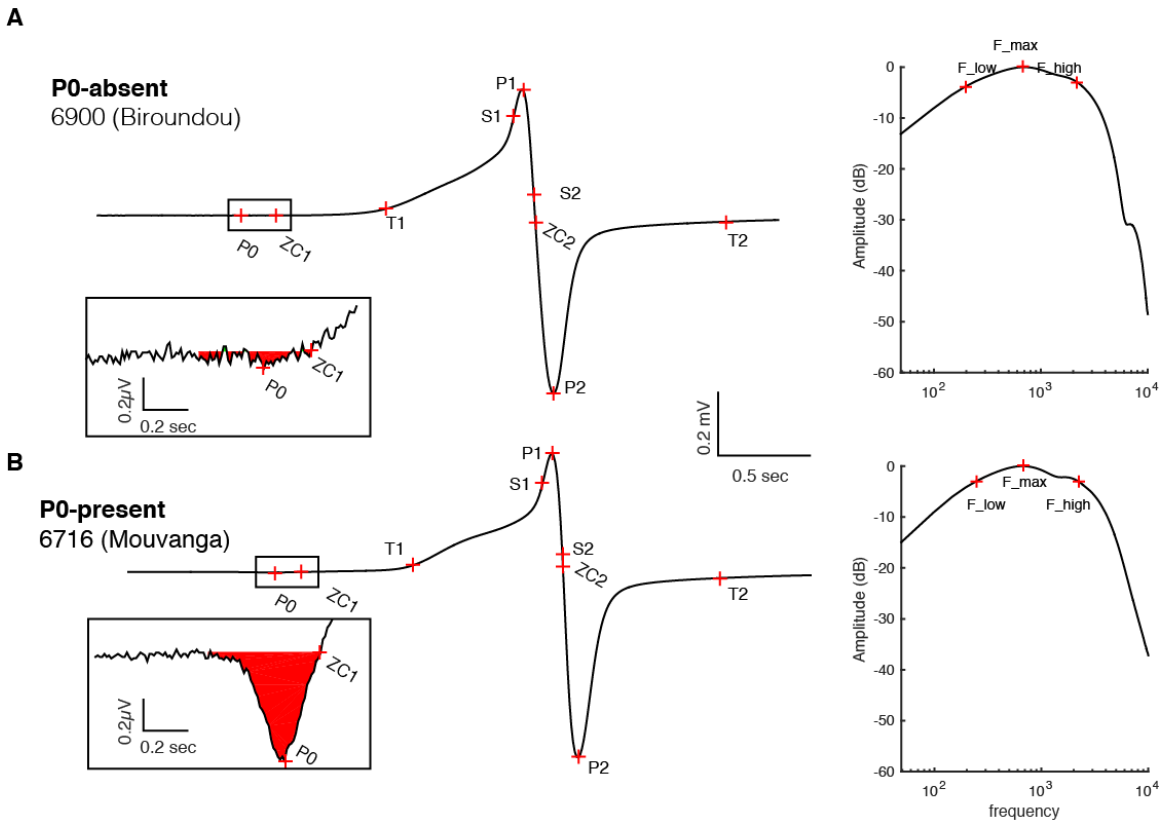

Figure 3. Example EOD Waveforms and Landmarks Measured.
EOD landmarks and measurements used in this analysis were identical to those described in Gallant *et al*. (2011) and are listed for the reader's convenience as Table 3. We indicate two example EOD waveforms: P0-absent (**A**) and P0-present (**B**) to illustrate the locations of these landmarks on EOD waveforms and their associated power spectra.

Landmarks		
	Name	*Definition*
	P0	Small negative pre-potential; assumed present in all waveforms
	P1	Largest head positive phase
	P2	Largest head negative phase
	S1	Point of maximum slope between T1 and P1
	S2	Point of maximum slope between P1 and P2
	T1	Waveform beginning; first point to deviate from baseline by 2% of peak to peak height
	T2	Waveform ending; last point to deviate from baseline by 2% of peak to peak height
	ZC1	Point voltage crosses baseline from P1-start of record; if exists
	ZC2	Point voltage crosses baseline between P1-P2
Variables		
	Name	*Definition*
	aP0	Area under curve between ZC1-0.5ms and ZC1
	aP1	Area under curve between ZC2-ZC1
	aP2	Area under curve between tT2-ZC2
	vP0	Minimum voltage between ZC1-0.5ms and ZC1
	vP1	Voltage of P1 (vP1-vP2=1)
	vS1	Voltage at S1
	vS2	Voltage at S2
	tP0	Time at P0
	tP2	Time at P2
	tS1	Time at S1
	tS2	Time at S2
	tZC1	Time at ZC1
	tZC2	Time at ZC2
	Duration	Total duration (T2-T1)
	sZC1	Slope at ZC1
	sZC2	Slope at ZC2
	sS1	Slope at S1
	sS2	Slope at S2
	fftmax	Peak frequency of FFT transform of EOD
	fftlo	Frequency below fftmax at -3dB
	ffthi	Frequency above fftmax at -3dB

Table 2. Landmark and variable definitions each of the landmarks used for EOD analysis are defined. All variables used in subsequent PCA are defined using these landmarks.

	NBB01				NBB02				NBB03				NBB04				NBB05			
Pop.	***k***	***Ho***	***He***	***p***	***k***	***Ho***	***He***	***p***	***k***	***Ho***	***He***	***p***	***k***	***Ho***	***He***	***p***	***k***	***Ho***	***He***	***p***
Apassa	6	0.71	0.67	0.955	4	0.79	0.71	0.393	6	0.75	0.68	0.212	4	0.64	0.75	0.276	17	0.75	0.92	0.184
Bale	5	0.55	0.63	0.552	10	0.64	0.87	0.015	10	0.82	0.88	0.422	6	0.55	0.58	0.143	9	0.73	0.88	0.445
Bambomo 09	6	0.38	0.35	0.963	11	0.82	0.75	0.114	7	0.69	0.69	0.393	11	0.37	0.62	0.000	21	0.72	0.78	0.174
Bavavela	6	0.67	0.60	0.693	6	0.58	0.59	0.184	6	0.83	0.81	0.546	4	0.83	0.73	0.059	6	0.71	0.71	0.584
Bambomo 99	5	0.41	0.38	0.537	5	0.67	0.77	0.251	4	0.44	0.63	0.003	4	0.22	0.69	0.000	4	0.78	0.81	0.455
Bikagala	2	0.69	0.64	0.485	3	0.52	0.53	0.120	5	0.52	0.59	0.437	6	0.34	0.33	0.373	3	0.55	0.54	0.038
Mouvanga 09	4	0.09	0.09	1.000	7	0.16	0.15	1.000	5	0.44	0.42	0.811	8	0.44	0.43	0.445	13	0.44	0.51	0.576
Mouvanga 99	2	0.05	0.05	1.000	3	0.16	0.15	1.000	5	0.32	0.37	0.147	6	0.37	0.48	0.228	4	0.63	0.56	0.644
Nyamé Pendé	4	0.17	0.31	0.090	11	0.58	0.88	0.019	8	1.00	0.85	0.173	4	0.08	0.60	0.000	13	1.00	0.93	1.000
Okano	8	0.53	0.55	0.271	2	0.24	0.25	0.569	7	0.42	0.37	1.000	9	0.45	0.43	0.489	16	0.82	0.90	0.197
Songou	3	0.33	0.52	0.202	2	0.11	0.11	1.000	4	0.33	0.65	0.090	2	0.22	0.52	0.172	2	0.22	0.21	1.000

Table 3 Summary of loci attributes.
For each locus and population, the number of alleles (k) at each locus, the observed (H_o) and expected heterozygosity (H_e) are reported. Probabilities of deviation from HWE are reported as p.

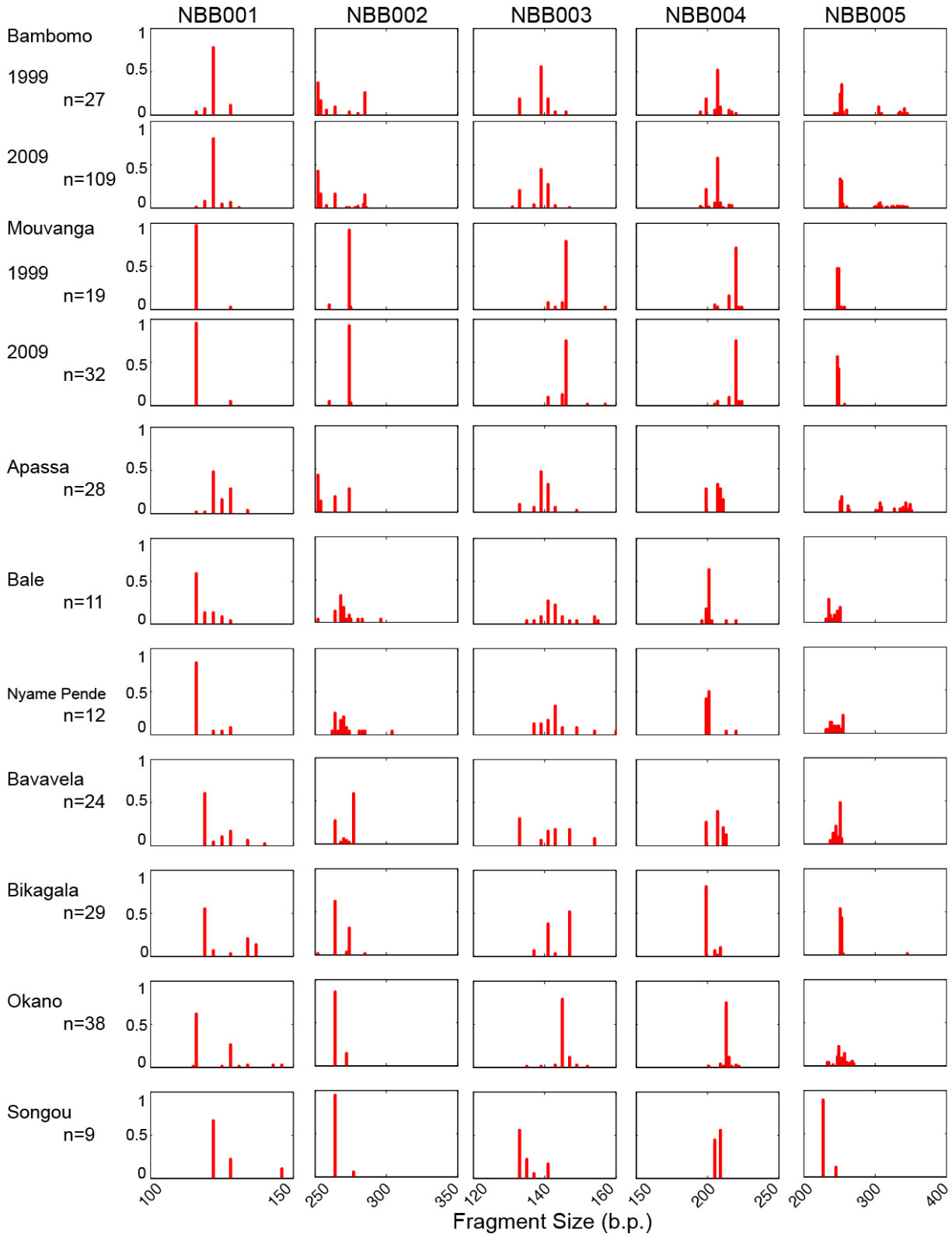
NBB001
NBB002
NBB003
NBB004
NBB005
Bambomo
1999
n=27
2009
n=109
Mouvanga
1999
n=19
2009
n=32
Apassa
n=28
Bale
n=11
Nyame Pende
n=12
Bavavela
n=24
Bikagala
n=29
Okano
n=38
Songou
n=9
1
0.5
0
100
150
250
300
350
120
140
160
150
200
250
200
300
400
Fragment Size (b.p.)

Figure 4. Allele frequency histograms for each population and microsatellite locus.
Microsatellite loci were designated as NBB001-NBB005 by Arnegard et al. (2005). For each population, sample sizes are reported as number of individuals genotyped, so the plots include twice as many allele copies.

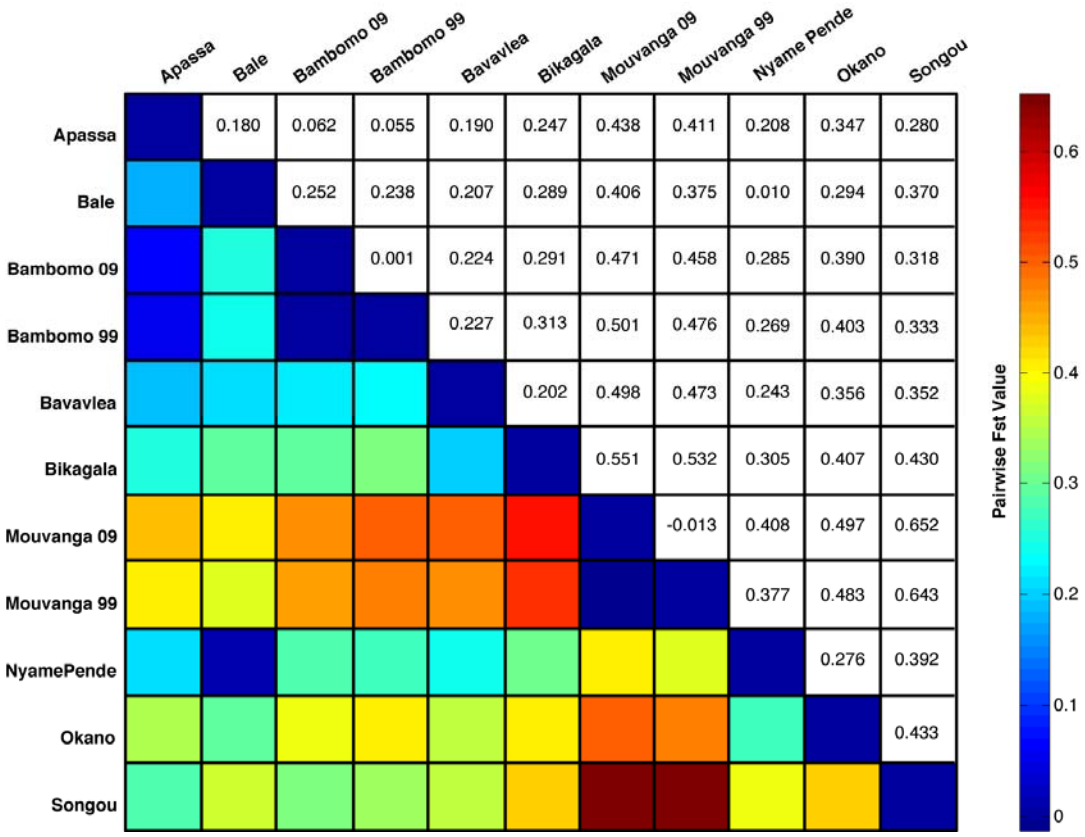

Figure 5 F_{st} values for each pairwise comparision of populations. Lower half of the matrix codes F_{st} value by color, the upper half of the matrix reports the individual F_{st} values. All pairwise comparisions of F_{st} values were significant at Bonferonni-corrected thresholds, with the exception of Mouvanga Creek (1999 vs. 2009), Bambomo Creek (1999 vs. 2009), and Bale Creek vs. Nyamé Pendé Creek.

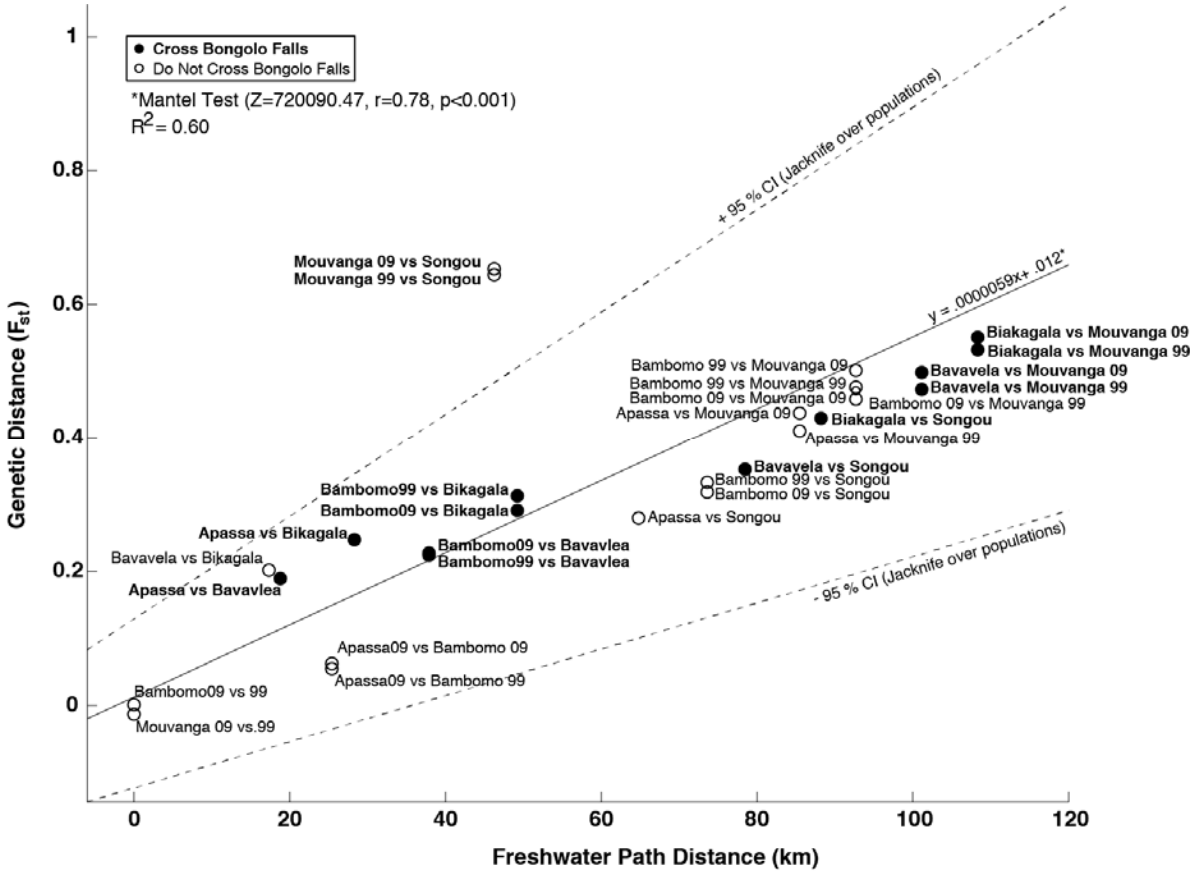

Figure 6 Comparison of pairwise F_{st} values and geographic distances in Southern Populations.

Geographic distance was measured as the shortest river distance between two populations. In some pairwise comparisons, this distance traversed Bongolo Falls, and in others it did not. The two types of distances are indicated as closed and open circles respectively. RMA regression was computed for the relationship between genetic and geographic distance, and the significance of the relationship between geographic and genetic distance was evaluated using a Mantel test (see results). 95% confidence intervals, computed by one-delete jackknifing (Bohonak 2002) across populations are shown as dashed lines.

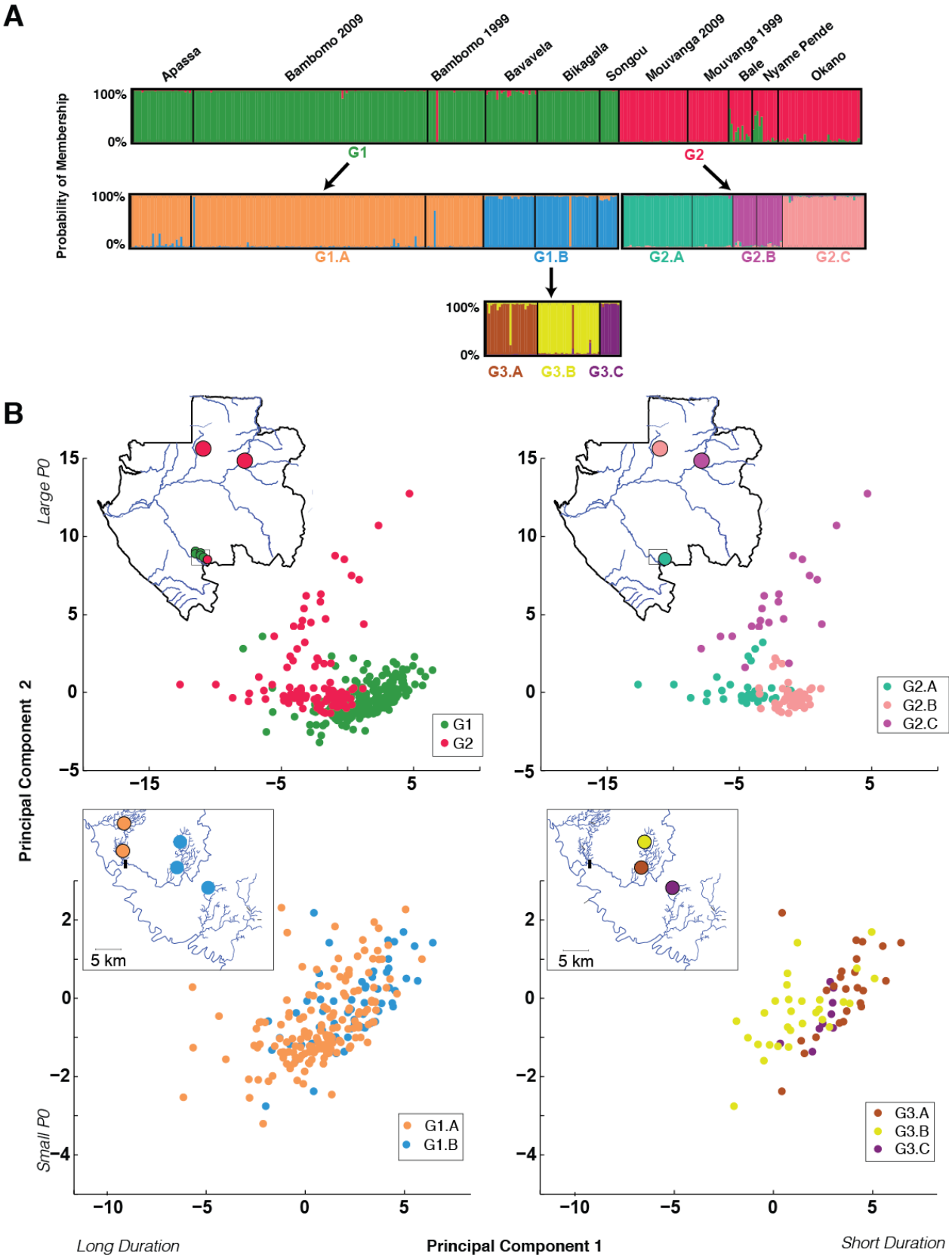
A
Apassa
Bambomo 2009
Bambomo 1999
Bavavela
Bikagala
Songou
Mouvanga 2009
Mouvanga 1999
Bale
Nyame Pende
Okano
Probability of Membership
100%
0%
G1
G2
G1.A
G1.B
G2.A
G2.B
G2.C
G3.A
G3.B
G3.C
B
Large P0
Small P0
Principal Component 2
Principal Component 1
Long Duration
Short Duration
5 km
G1
G2
G2.A
G2.B
G2.C
G1.A
G1.B
G3.A
G3.B
G3.C

Figure 7. Genetic structure and signal variation.
STRUCTURE analysis was performed hierarchically using the methods of Evanno et al. (2005), see text. (A) Individuals are represented on a bar chart with the probability of membership to each group (below) is indicated by the color of each bar. Populations are separated by black lines. G1 and G2 were subdivided and analyzed for population substructure, and individuals are shown with their probability of membership in each subgroup. Subgroup G1.B. was further analyzed, and found to subdivide into 3 distinct subgroups. Note the correspondence between sampling populations and genetic grouping, except for Bambomo and Apassa Creek, which are indistinguishable genetically. (B) Variation in EOD signals was quantified using Principal Components Analysis (see Gallant et al., 2011 and text for further details). Principal component 1 strongly loaded duration, whereas principal component 2 strongly loaded P0 magnitude and some with duration (see Table 4). Insets indicate the geographic location of each genetic cluster on map of Gabon in the top two panels, and detail of the confluence of the Ngounié and Louétsi rivers in the lower two panels. Top left shows correspondence between G1 and G2 and EOD signal types (P0 absent and P0 present). Top right shows correspondence among genetic and signal differences among G1 and variation in duration and P0 magnitude. Lower left, represents the two subclusters of G1, which show considerable overlap both in both duration and P0 magnitude. Lower right, representing the three subclusters of G1B shows some correspondence of genetic clustering and duration, but not P0 magnitude.

Variable	PC1	PC2
Duration	-0.231039624	-0.154355104
tS0	9.15E-17	-2.43E-17
vs0	4.99E-18	-5.12E-17
sS0	8.92E-19	-2.06E-17
tP0	0.007062138	0.215129534
vP0	0.154756171	-0.388112877
tZC1	-0.000420046	0.217966522
sZC1	-0.12366472	0.029885385
tS1	0.195135682	0.186615757
vS1	-0.269027139	0.127344811
sS1	0.186298317	-0.265371541
tS2	-0.303830145	-0.033700684
vS2	-0.008076105	0.061480219
sS2	-0.203426695	0.312642581
tZC2	-0.314780611	-0.003276516
sZC2	-0.20730134	0.310600964
tP2	-0.312460562	-0.014781453
F_Low	0.166464022	0.37268552
F_Max	0.164288193	0.394851868
F_High	0.320361843	0.07724885
ap0	0.11934371	-0.292851849
ap1	-0.327003105	-0.128118623
ap2	0.331976479	0.084177515

Table 4. Summary of Factor Loadings for Principal Components Analysis. Variables measured in this analysis were described in detail in Table 3.

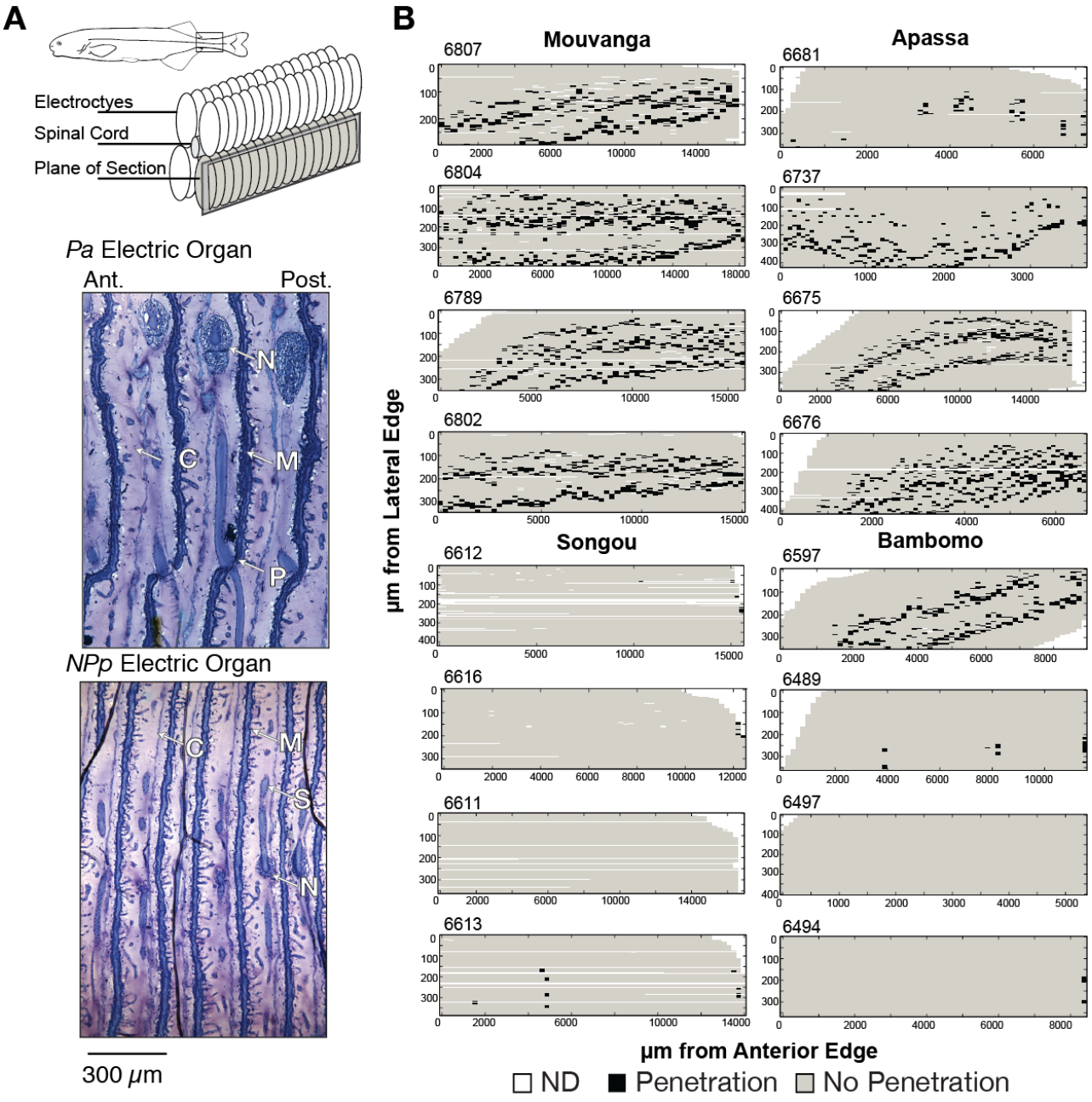
A
Electroctyes
Spinal Cord
Plane of Section
Pa Electric Organ
Ant.
Post.
N
C
M
P
NPp Electric Organ
C
M
S
N
300 μm
B
Mouvanga
Apassa
Songou
Bambomo
6807
6804
6789
6802
6612
6616
6611
6613
6681
6737
6675
6676
6597
6489
6497
6494
μm from Lateral Edge
μm from Anterior Edge
ND
Penetration
No Penetration

Figure 8. Summary of histological survey of electric organs. **A.** Individual *P. kingsleyae* were sectioned sagittally from lateral to medial, following one column of electrocytes of the 4 that comprise the electric organ. The electric organ is restricted to the caudal peduncle in mormyrids. Example histology showing the two basic types of anatomical configuration in the electric organ *Pa* (penetrating with anterior innervation) and NPp (nonpenetrating with posterior innervation). Stalks (S) can be seen clearly passing through the electrocyte penetrations (P) in Pa but not in NPp type electrocytes. Microstalklets (M) can be observed on the posterior face in both cases, and connective tissue boundaries (C) bounding each electrocyte are indicated. Innervation (N) can be observed on the anterior or posterior side of the electrocyte accordingly. Pa type electrocytes result in EOD signals that have a small head negative phase P0, which is absent in individuals with electrocytes that are NPp (see Gallant et al., 2011). **B.** Examples of histological analysis of 4 electric organs from each population. Each pixel represents an individual electrocyte in an individual section that was scored for presence of penetrations (black). In Apassa creek, most individuals have Pa type observed in each electrocyte from anterior to posterior, whereas one individual had NPp type and Pa type electrocytes (patches of black in mostly grey background). In Bambomo, most individuals were NPp with one individual exhibiting all Pa type electrocytes. Songou was entirely comprised of individuals with NPp type electrocytes, and Mouvanga was comprised of individuals with entirely Pa type electrocytes. Full analysis is summarized in Table 5.

Population	Specimen No.	µm Surveyed	No. Sections	No. Electrocytes	No. *Pa*	No. *NPp*	Morphology
Apassa	6681	420	70	60	15	45	Mixed
Apassa	6675	648	108	64	50	14	Pa
Apassa	6676	366	61	69	58	11	Pa
Apassa	6637	258	43	70	65	5	Pa
Bambomo	6489	240	40	60	10	50	NPp
Bambomo	6494	384	64	61	1	60	NPp
Bambomo	6497	276	46	67	0	67	NPp
Bambomo	6500	270	45	59	1	58	NPp
Bambomo	6547	378	63	52	1	51	NPp
Bambomo	6549	186	31	60	5	55	NPp
Bambomo	6597	438	73	58	43	15	Pa
Mouvanga	6789	516	86	58	53	5	Pa
Mouvanga	6811	342	57	62	55	7	Pa
Mouvanga	6807	582	97	50	49	1	Pa
Mouvanga	6810	390	65	66	61	5	Pa
Mouvanga	6804	570	95	65	65	0	Pa
Mouvanga	6802	570	95	57	57	0	Pa
Songou	6611	252	42	59	0	59	NPp
Songou	6612	564	94	70	4	66	NPp
Songou	6613	234	39	64	5	59	NPp
Songou	6616	480	80	57	2	55	NPp

Table 5. Summary of electric organ histological survey, performed on 21 specimens of *Paramormyrops kingsleyae*.
For each individual, the collection locality and specimen number are provided. For each specimen, one column of the entire electric organ was surveyed for the specified depth (µm) from lateral to medial (see Fig. 6). Total number of electrocytes, and the number of those exhibiting *Pa* type morphology and *NPp* type morphology are provided. Finally, the assessment of the overall EO morphology is specified as either Pa (nearly all electrocytes Pa) NPP (nearly all electrocytes NPp) or mixed (some electrocyes NPp some Pa). Note that some individuals determined to have Pa anatomy did not have penetrations in the rostral or caudal portion of the organ (See Fig. 8). In these cases, electrocytes could not be fully surveyed because of the orientation of tissue during sectioning.

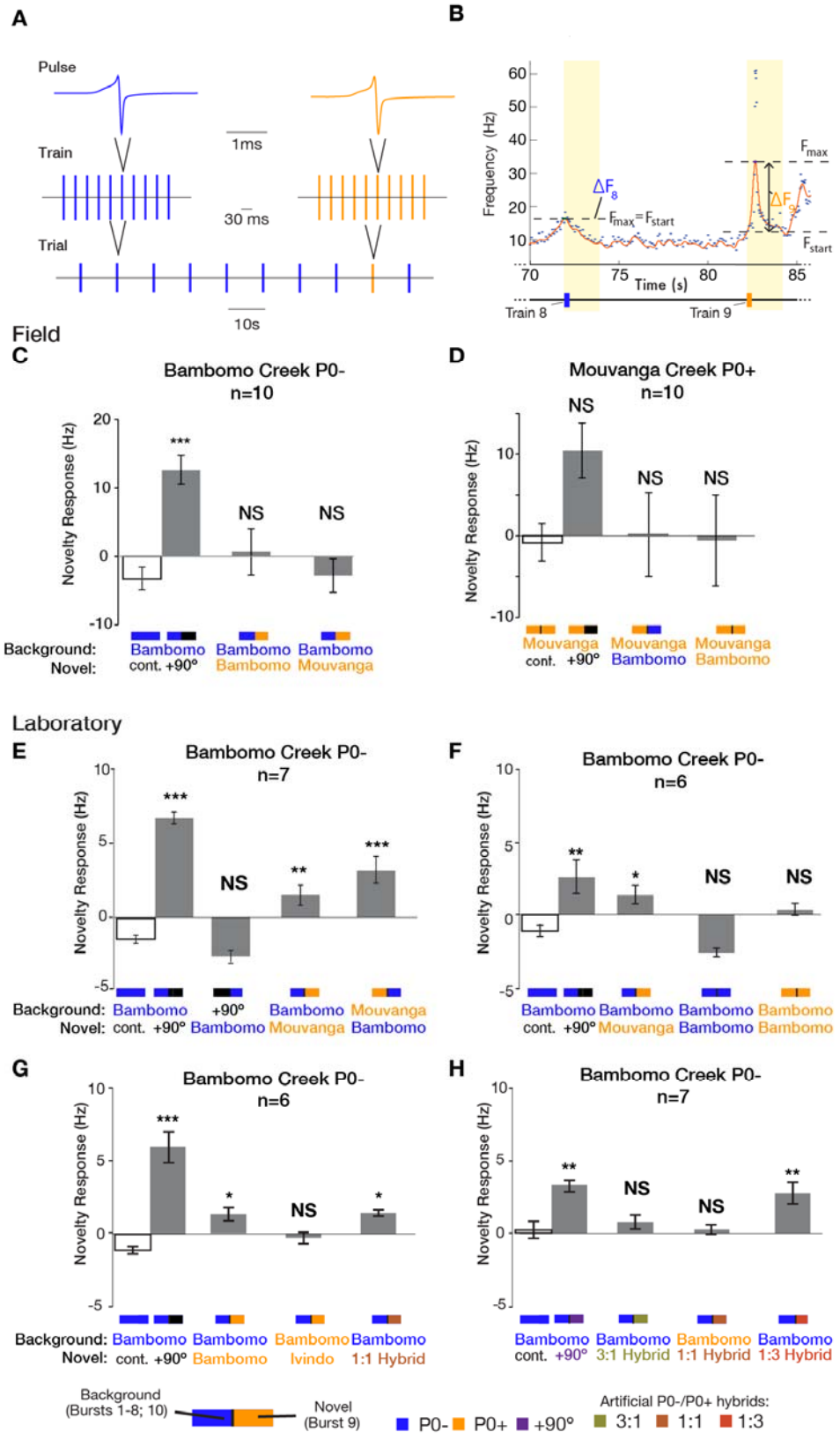
A
Pulse
Train
Trial
1ms
30 ms
10s
B
Frequency (Hz)
Time (s)
Fmax
Fstart
ΔF8
ΔF9
Fmax=Fstart
Train 8
Train 9
Field
C
Bambomo Creek P0-
n=10
Novelty Response (Hz)
Background:
Novel:
Bambomo
cont. +90°
Bambomo
Bambomo
Bambomo
Mouvanga
D
Mouvanga Creek P0+
n=10
Mouvanga
cont. +90°
Mouvanga
Bambomo
Mouvanga
Bambomo
Laboratory
E
Bambomo Creek P0-
n=7
Background: Bambomo +90° Bambomo Mouvanga
Novel: cont. +90° Bambomo Mouvanga Bambomo
F
Bambomo Creek P0-
n=6
Bambomo Bambomo Bambomo Bambomo
cont. +90° Mouvanga Bambomo Bambomo
G
Bambomo Creek P0-
n=6
Background: Bambomo Bambomo Bambomo Bambomo
Novel: cont. +90° Bambomo Ivindo 1:1 Hybrid
H
Bambomo Creek P0-
n=7
Bambomo Bambomo Bambomo Bambomo
cont. +90° 3:1 Hybrid 1:1 Hybrid 1:3 Hybrid
Background
(Bursts 1-8; 10)
Novel
(Burst 9)
P0- P0+ +90°
Artificial P0-/P0+ hybrids:
3:1 1:1 1:3

Figure 9. Playback experiments performed on *P. kingsleyae* A. Stimuli used: 10 presentations (trains) of 10 waveform pulses were presented in each trial. 9 trains were comprised of one waveform type (background) and one train was comprised of a second waveform type (novel). B. Example of subject response. Subject's EOD discharges were continuously monitored (black dots), and discharge frequency was fitted with a spike density function (red line). The maximum and starting discharge rate of the SDF was calculated over the 2sec interval from the onset of each train presentation. The difference between these values defined the change in frequency (ΔF) for that train. Novelty response was defined as the difference in ΔF between the 8th and 9th (novel) train presentation. See methods for details. C-D Experiments performed on field captured specimens, G-H Experiments performed in the laboratory. Subjects and sample sizes are described in italics above each plot. Bars show mean novelty responses averaged for all specimens. Subtext indicates the localities where background and novel waveforms were recorded, if applicable. Stars reflect significance as compared to negative control (Dunnett's Test w/Control: NS: not significant, * $p=0.05$; ** $p<0.01$; *** $p<0.001$.